Supersonic Reacting Internal Flow Fields

J. Philip Drummond*

The national program to develop a trans-atmospheric vehicle has kindled a renewed interest in the modeling of supersonic reacting flows, both in the United States and abroad. A supersonic combustion ramjet, or scramjet, has been proposed to provide the propulsion system for this vehicle. Work has been underway for the past 25 years to develop and optimize a scramjet propulsion system for a variety of purposes, but during most of this period, the program has not reached the level of intensity that it currently enjoys. With the maturing of the scramjet development program, techniques to model the engine flow field have also progressed significantly. This has been due both to an advancement in numerical methods for computing reacting flow fields as well as an appreciable growth in computer speed and storage. The improvements in both algorithms and computer power have also lead to a gradually improved understanding of the physics of reacting flow fields which is so very important if computation is to have a truly significant impact on scramjet design. This chapter will deal principally with the development of computational techniques for modeling supersonic reacting flow fields, and the application of these techniques to an increasingly difficult set of combustion problems. Since the scramjet problem has been largely responsible for motivating this computational work, we will begin with a brief history of hypersonic vehicles and their propulsion systems. This will be followed by a discussion of some early modeling efforts applied to high speed reacting flows. We will then move to the present day and discuss current activities to develop accurate and efficient algorithms and improved physical models for modeling supersonic combustion. Following

*Senior Research Scientist, Computational Methods Branch, Fluid Mechanics Division, NASA Langley Research Center, Hampton, Virginia 23665. Phone (804) 864-2298. Associate Fellow, AIAA.

that discussion, some new problems where computer codes based on these algorithms and models are being applied will be described. We will then be ready to look beyond the current day and draw some conclusions concerning future needs and directions for modeling supersonic reacting flows, and hopefully challenge the reader to tackle one of these exciting problems that we face in the future.

Introduction

Research to develop a supersonic combustion ramjet, or scramjet, propulsion system was underway in the late 1950's. In unrelated efforts, work had also begun to develop computational techniques for solving the equations governing the flow through a scramjet engine. The marriage of scramjet technology and computational methods for assisting in its evolution would remain apart for another decade, however. The principle barrier to the union was the lack of a high-speed computer technology for solving the discrete equations provided by the numerical methods. Computer resources remain even today as a major pacing item in overcoming this barrier. Significant advancement has been made over the past thirty years, however, to model the supersonic chemically reacting flow in a scramjet combustor. To see how the the two fields finally merged, it is useful to briefly trace the evolution of the technology in both areas.

Following a moderate level of activity in the late 1950's, there was a significant increase in the research to develop scramjet engine concepts in the 1960's. In 1965, the NASA Langley Research Center initiated the Hypersonic Research Engine (HRE) Project to develop a high speed airbreathing technology base that could then be applied to the development of propulsion systems for hypersonic cruise vehicles [1]. The goal of the HRE Project was to flight test a regeneratively cooled, hydrogen fueled, pilon mounted scramjet on the X-15 research airplane and demonstrate design performance levels. The HRE did not reach the flight demonstration stage due to cancellation of the X-15 program, but the ground based program did continue and resulted in the development and construction of

two variable geometry engine models. Work with these models significantly increased the scramjet technology base to be applied in more advanced configurations.

Following completion of the HRE Project, attention moved to propulsion concepts that would provide high performance when installed on a vehicle. The pilon mounted HRE would have resulted in excessive levels of external drag, so the pilon was removed and work began to highly integrate the engine with the airframe of candidate vehicles. In addition, engine weight was reduced by moving from a variable to a fixed geometry which reduced the amount of engine structure. Out of this activity, the Langley airframe integrated scramjet engine concept was conceived. That program, which has continued to the present day, resulted in the successful demonstration of the concept to produce net thrust in subscale hardware. A detailed review of this program was given by Northam et al. in reference [1], and the reader is referred to their discussion for further details.

In addition to the NASA scramjet research and development program, other government activities included a Navy sponsored scramjet program at the Applied Physics Laboratory of the Johns Hopkins University (JHU/APL) [2,3]. This work also increased in the 1960's and was directed towards the development of an air-breathing shipboard missile utilizing a scramjet propulsion system. Development of this concept continued until 1977. At that time, concern over the storage of highly reactive and toxic fuels to be used by the system forced a change to more conventional but safer fuels. This change resulted in the development of an integral rocket/duel combustor ramjet concept that utilized a fuel-rich gas generator to preburn the fuel for a main supersonic combustor, thus allowing the use of hydrocarbon fuels [4].

The Air Force also sponsored scramjet research and development during the 1960's [2]. They continued the support of several programs that were initially funded by the HRE program. In 1964, a program was started at the General Applied Science Laboratory to continue development of a low-speed fixed geometry scramjet engine, and a duel-mode scramjet program was continued with the Marquardt Company at the same time. Soon

thereafter in 1965, the Air Force began an effort with the United Aircraft Research Laboratory to continue development of a water cooled variable geometry scramjet design. These three efforts ended in 1968, and only the NASA and JHU/APL programs continued into the 1970's.

It was also during the 1970's that computational techniques were first applied to study the supersonic reacting flow found in a scramjet combustor. A detailed review of those activities was given by White, et al. in reference [2], and a summary of that discussion and additional work is now provided. Some of the earliest work to model supersonic reacting flows was undertaken by Ferri [5] and his colleagues, Morretti [6], Elelman [7], and Dash [8,9]. They employed an explicit viscous characteristics method that split the governing equations into hyperbolic and parabolic parts followed by a coupled numerical solution of each part at each integration step. Modeling of multistep finite rate chemistry was also included in their solution strategy. Spalding and his colleagues then took Ferri's splitting-based approach and improved its efficiency by developing a fully implicit solution procedure for solving the governing equations [10]. Spalding then developed several implicit parabolized Navier-Stokes programs for modeling scramjet combustor flow fields. These codes included the CHARNAL two-dimensional axisymmetric program [11] and the SHIP three-dimensional program [12]. Both programs utilized the well known SIMPLE solution procedure for spatially marching the governing equations in the parabolized direction while employing a tri-diagonal matrix solution procedure to perform repetitive sweeps for solution of the equations in the cross-plane(s) [13]. The programs were written to assume that a state of chemical equilibrium alway existed, but they were later modified by Evans [14] to include the effects of finite rate chemical reactions. The modified programs are still being used today for studies of mixing and reaction in candidate combustor configurations.

The work of Ferri and Spalding was then adapted by Dash to develop the SCORCH program that used a hybred explicit/implicit procedure for modeling supersonic reacting

flows. The method again split the governing equations into hyperbolic and parabolic parts. The hyperbolic part was solved using a viscous characteristics approach that employed an upwind finite difference procedure. The parabolic part was solved using an implicit finite difference procedure [15]. Work on this program and its application to supersonic combustion problems has continued to the present day.

While Ferri, his colleagues, and Spalding were developing analysis techniques for direct application to the supersonic reacting flow problem in a scramjet, other algorithm development work was underway, directed primarily at solving high speed external flow problems. These techniques ultimately found their way, however, into the internal reacting flow arena. The first of these algorithms was the MacCormack explicit, unsplit predictor-corrector method that was initially developed to model the hypervelocity impact cratering problem [16]. The MacCormack method was a variation of the Lax-Wendroff second order accurate scheme. The method was robust and easily applied to complex geometries. Because of these qualities, the algorithm was readily adopted and used to study a wide class of external flow problems. In fact, due to its general applicability, MacCormack's unsplit algorithm is still used today as one option in several codes that are applied extensively to the modeling of scramjet flow fields. Implicit algorithms were also developed for external flow problems in the 1970's. Their development was motivated by the need to resolve the high gradients present in wall boundary layers. The resolution of boundary layers required fine computational grids, resulting in a severe stability constraint on the marching step size of an explicit method. Where only a steady state solution was required, i.e., time accuracy was not necessary, implicit methods could achieve a significantly more rapid rate of convergence. Early work to develop implicit solution techniques for the Navier-Stokes equations was carried out by Briley and McDonald [17] and Beam and Warming [18]. Both approaches used a spatial factoring procedure that reduced the multidimensional problem to one of sequentially solving a set of one dimensional spatial implicit operators. Using this computationally efficient procedure, convergence rates one to two orders of mag-

nitude faster than the explicit method were achieved for steady-state problems on highly stretched grids.

While the application of implicit methods was generally limited to scramjet inlet flow fields through the late 1970's and early 1980's, explicit methods were applied extensively in studies of combustor flow fields. The MacCormack method was employed by Drummond to model internal scramjet combustor flow fields. In 1977, he developed the two-dimensional TWODLE combustion program based on that method. The code used an equilibrium chemistry scheme to model H_2-air reaction and several algebraic eddy viscosity methods to model the turbulence field. The program was applied to several scramjet combustor component problems. Particular emphasis was given to the scramjet fuel injector problem in an attempt to better understand the complex flow field in this region of the engine [19,20]. Development on the program continued into the early 1980's when the program was used to carry out the first simulation of a scramjet flow field using a two-dimensional model engine module [22]. Detailed studies to optimize candidate scramjet fuel injector configurations were also completed during this period [21,23].

An explicit solution procedure was also employed by Schetz during the early 1980's to model the APL duel combustion ramjet described earlier [26]. He employed a modular approach to carry out his analysis. The mixing and burning of the center jet from the fuel-rich gas generator was calculated with a jet mixing code [24,25] that was modified to include a turbulent kinetic energy turbulence model, a chemistry model, and other improvements. Because of the high static pressures and temperatures that were present in the device, a local diffusion-controlled, equilibrium chemistry model was used to model reaction in the combustor. Schetz's procedure for modeling combustor flows was ultimately combined with an inlet analysis procedure to compute performance estimates for the duel combustion ramjet [27].

While numerical methods for modeling scramjet flow fields were developing through the 1960's, 1970's and early 1980's, there was a parallel growth in computer hardware

upon which these methods could be applied. Many of the early calculations were carried out on IBM 7090 and CDC 6600 class machines. Hardware improvements, that allowed the consideration of more realistic problems came in the late 1960's with the arrival of the CDC 7600 computer. The most significant hardware improvement came in the mid and late 1970's, however, when vector processing supercomputers became available to the computational community. These machines included the CDC Star-100 and the Cray 1. They were followed in the early 1980's by the Cyber 205 and the Cray X-MP which gave performance capabilities several orders of magnitude greater than the scalar machines available to the researcher prior to their arrival [2]. To this time, the state of computer resources had resulted in a major barrier to advancing the state of the art in modeling supersonic reacting flows. With the new machines, however, the researcher was now in a position to begin dealing with the detailed physics contained in these complex flows. The burden now returned *partially* to the state of numerical algorithms used to model supersonic combustion. This state has continued to the present day.

We are now in a situation where both numerical algorithms and computer technology are pacing our ability to formulate an improved understanding of supersonic reacting flows. We will concentrate for the remainder of this chapter on the numerical challenge, i.e. what is needed to advance the computational state of the art that will result in an improved understanding of supersonic reacting flows. We will then explore how we can use this improved understanding to solve practical problems associated with the modeling and design of a scramjet combustor. There is a critical need today for creditable methods for modeling flows typical of those found in a supersonic combustor. The National Aero-Space Plane, mentioned earlier in this chapter, will operate at Mach numbers as high as 25. To develop a successful design for the propulsion system of this vehicle, extensive use will be made of ground-based facilities to create flow fields consistent with those that the engine will injest over its operating envelope. Unfortunately, however, ground based facilities are only able to create continuous flow conditions up to a flight Mach number of about

8. Beyond Mach 8, the only options available to the experimentalist are pulse facitities that create flight conditions for only a short period of time, providing a data collection window of only a few milliseconds. Numerical methods provide an alternative to the Mach 8 barrier, but only if they are properly applied to the problem. To examine the challenge that this poses for those who are applying computational methods, we will proceed along the following path. We will first review the equations that govern the supersonic reacting flow problem and the modeling that these equations require. We will next explore a number of promising numerical methods, both old and new, for accurately solving these governing equations. Several solutions for reacting flow problems using some of these methods will then be presented to assess the capabilities of the techniques and the computers which provided their results. We will then be in a position to evaluate where we are with these methods and where we need to go. That will be the subject of the conclusion to this chapter, or at least this author's perspective of it!

Theory

Governing Equations

The Navier-Stokes, energy, and species continuity equations governing multiple species undergoing chemical reaction have been derived by Williams [28]. The terms used in these and subsequent equations are defined in the appendix at the end of this chapter. The governing equations are given by

Continuity

$$\frac{\partial \rho}{\partial t} + \nabla \cdot (\rho \vec{V}) = 0 \tag{1}$$

Momentum

$$\frac{\partial (\rho \vec{V})}{\partial t} + \nabla \cdot (\rho \vec{V} \vec{V}) = \nabla \cdot \tau + \rho \sum_{i=1}^{ns} f_i \vec{b}_i \tag{2}$$

Energy

$$\frac{\partial(\rho E)}{\partial t} + \nabla \cdot (\rho \vec{V} E) = \nabla \cdot (\tau \cdot \vec{V}) - \nabla \cdot \vec{q} + \rho \sum_{i=1}^{ns} f_i \vec{b}_i (\vec{V} + \tilde{V}_i) \tag{3}$$

Species Continuity

$$\frac{\partial(\rho f_i)}{\partial t} + \nabla \cdot (\rho \vec{V} f_i) = \dot{w}_i - \nabla \cdot (\rho f_i \tilde{V}_i) \tag{4}$$

where

$$\tau \equiv \tau_{ij} = -\delta_{ij} p + \mu \left(\frac{\partial u_i}{\partial x_j} + \frac{\partial u_j}{\partial x_i}\right) + \delta_{ij} \lambda \frac{\partial u_k}{\partial x_k} \tag{5}$$

and

$$\vec{q} = -k \nabla T + \rho \sum_{i=1}^{ns} h_i f_i \tilde{V}_i + R^o T \sum_{i=1}^{ns} \sum_{j=1}^{ns} \left(\frac{X_j D_{T_i}}{M_i D_{ij}}\right)(\tilde{V}_i - \tilde{V}_j) \tag{6}$$

Radiation heat transfer is not included in equation (6). Also,

$$E = \sum_{i=1}^{ns} h_i f_i - \frac{p}{\rho} + \frac{u^2 + v^2}{2} \tag{7}$$

$$h_i = h_i^o + \int_{T_r}^{T} c_{p_i} dT \qquad i = 1, 2, ..., ns \tag{8}$$

$$p = \rho R^o T \sum_{i=1}^{ns} \frac{f_i}{M_i} \tag{9}$$

The diffusion velocities are found by solving

$$\nabla X_i = \sum_{j=1}^{ns} \frac{X_i X_j}{D_{ij}} (\tilde{V}_j - \tilde{V}_i) + (f_i - X_i) \frac{\nabla p}{p} + \frac{\rho}{p} \sum_{j=1}^{ns} f_i f_j (\vec{b}_i - \vec{b}_j) + \sum_{j=1}^{ns} \frac{X_i X_j}{\rho D_{ij}} \left(\frac{D_{Tj}}{f_j} - \frac{D_{Ti}}{f_i}\right) \frac{\nabla T}{T} \tag{10}$$

Note that if there are ns chemical species, then i = 1,2,...,(ns-1) and (ns-1) equations must be solved for the species f_i. The final species mass fraction f_{ns} can then be found by conservation of mass since $\sum_{i=1}^{ns} f_i = 1$.

Thermodynamics Model

To calculate the required thermodynamic quantities, the specific heat for each species is first defined by a fourth-order polynomial in temperature

$$\frac{c_{p_i}}{R} = A_i + B_i T + C_i T^2 + D_i T^3 + E_i T^4 \tag{11}$$

The coefficients are found by a curve fit of the data tabulated in reference [29]. Knowing the specific heat of each species, the enthalpy of each species is then found from equation (8) and the total internal energy is computed from equation (7).

To determine the equilibrium constant (required in the next section) for each chemical reaction being considered, the Gibbs energy of each species must first be found. For a constant pressure process, $\frac{c_p}{T}$ from equation (11) is first integrated over temperature to define the entropy of the species, and then the resulting expression is integrated again over temperature to obtain a fifth-order polynomial in temperature for the Gibbs energy of each species.

$$\frac{g_i}{R} = A_i(T - T\ln T) + \frac{B_i}{2}T^2 + \frac{C_i}{6}T^3 + \frac{D_i}{12}T^4 + \frac{E_i}{20}T^5 + F_i - G_i T \tag{12}$$

The coefficients F_i and G_i are again defined in reference [29]. The Gibbs energy of reaction is then calculated as the difference between the Gibbs energy of product and reactant species.

$$\Delta G_{R_j} = \sum_{i=1}^{ns} \gamma''_{ji} g_i - \sum_{i=1}^{ns} \gamma'_{ji} g_i \qquad j = 1, 2, ..., nr \tag{13}$$

The equilibrium constant for each reaction can then be found from [30]

$$K_{eq_j} = \left(\frac{1}{R^o T}\right)^{\Delta n} \exp\left(\frac{-\Delta G_{R_j}}{R^o T}\right) \tag{14}$$

where Δn is the change in the number of moles when going from reactants to products.

Chemistry Models

The rate of reaction of chemical reactions is often defined by using the Arrhenius Law. A modified form of of the Arrhenius law is usually employed when modeling supersonic combustion. It is given by

$$K_{f_j} = A_j T^{N_j} \exp(\frac{-E_j}{R^o T}) \tag{15}$$

The values of the preexponential constant A, power constant N, and the activation energy E have been determined for a number of reaction schemes. Unfortunately, there is a great deal of uncertainty for many chemical reactions. One of the best understood mechanisms, however, is the hydrogen-air reaction system. This is not the reason that hydrogen fuel was chosen for several scramjet concepts, but it has proven convenient for its combustor analysists! Values for A, N, and E for a typical hydrogen-air mechanism are given in Table 1. Knowing the forward rate, the reverse rate is then given by

$$K_{b_j} = \frac{K_{f_j}}{K_{eq_j}} \tag{16}$$

Once the forward and reverse reaction rates have been determined, the production rates of the species are found from the law of mass action. For the general chemical reaction

$$\sum_{i=1}^{ns} \gamma'_{ji} C_i \overset{K_{f_j}}{\rightleftharpoons} \sum_{i=1}^{ns} \gamma''_{ji} C_i \qquad j = 1, 2, ..., nr \tag{17}$$

the law of mass action states that the rate of change of concentration of species i by reaction j is given by [28]

$$(\dot{C}_i)_j = (\gamma''_{ji} - \gamma'_{ji})[K_{f_j} \prod_{i=1}^{ns} C_i^{\gamma'_{ji}} - K_{b_j} \prod_{i=1}^{ns} C_i^{\gamma''_{ji}}] \qquad i = 1, 2, ..., ns \tag{18}$$

The net rate of change in concentration of species i by reaction j is then found by summing the contributions from each reaction

$$\dot{C}_i = \sum_{j=1}^{nr} (\dot{C}_i)_j \tag{19}$$

Finally, the production of species i can be found by multiplying its rate of change of concentration by its molecular weight.

$$\dot{w}_i = \dot{C}_i M_i \tag{20}$$

The source terms in equation (4) are now determined as a function of the dependent variables.

Molecular Diffusion Models

The coefficients governing the molecular diffusion of momentum, energy, and mass are determined from models based on kinetic theory. The set of models that is often used is now described. Individual species viscosities are computed form Sutherland's law

$$\frac{\mu}{\mu_o} = (\frac{T}{T_o})^{1.5} \frac{T_o + S}{T + S} \tag{21}$$

where μ_o and T_o are reference values and S is Sutherland's constant. These constants are tabulated for many species in references [31,32]. Once the viscosity of each species has been determined, the mixture viscosity is found from Wilke's law [33]

$$\mu_m = \sum_{i=1}^{ns} \frac{\mu_i}{1 + \frac{1}{X_i} \sum_{j=1, j \neq i}^{ns} X_j \phi_{ij}} \tag{22}$$

where

$$\phi_{ij} = [\frac{1 + (\frac{\mu_i}{\mu_j} \frac{\rho_j}{\rho_i})^{0.5} (\frac{M_i}{M_j})^{0.25}]^2}{\frac{4}{\sqrt{2}} (1 + \frac{M_i}{M_j})^{0.5}} \tag{23}$$

Species thermal conductivities are also computed from Sutherlands's law

$$\frac{k}{k_o} = (\frac{T}{T_o'})^{1.5} \frac{T_o + S'}{T + S'} \tag{24}$$

with different values of the reference values k_o and T_o' and the Sutherland's constant S'. These values are also tabulated for a number of species in references [31,32]. The mixture

thermal conductivity is computed using conductivity values for the individual species and Wassilewa's formula [34]

$$k_m = \sum_{i=1}^{ns} \frac{k_i}{1 + \frac{1}{X_i} \sum_{j=1, j \neq i}^{ns} X_j \phi'_{ij}} \tag{25}$$

where $\phi'_{ij} = 1.065\ \phi_{ij}$ and ϕ_{ij} is taken from equation (18).

For dilute gases, Chapman and Cowling used kinetic theory to derive the following expression for the binary diffusion coefficient D_{ij} between species i and j [31].

$$D_{ij} = \frac{0.001858 T^{1.5} \left(\frac{M_i + M_j}{M_i M_j}\right)^{0.5}}{p \sigma_{ij}^2 \Omega_D} \tag{26}$$

Here, the diffusion collision integral Ω_D is approximated by

$$\Omega_D = \bar{T}^{-0.145} + (\bar{T} + 0.5)^{-2} \tag{27}$$

where $\bar{T} = \frac{T}{T_{\epsilon_{ij}}}$. Values of the effective temperature T_ϵ and the effective collision diameter σ are taken to be averages of the separate molecular properties of each species, giving

$$\sigma_{ij} = 0.5(\sigma_i + \sigma_j) \tag{28}$$

and

$$T_{\epsilon_{ij}} = (T_{\epsilon_i} T_{\epsilon_j})^{0.5} \tag{29}$$

For most molecules, the thermal diffusion coefficient is generally small when compared with the binary diffusion coefficient, and therefore, the thermal diffusion coefficient can be neglected. This is a fortunate fact, since values of the thermal diffusion coefficient are generally not known for most species. For low molecular weight molecules such as hydrogen, though, the thermal diffusion coefficient can be important. A set of relationships for the thermal diffusion coefficient of species having a molecular weight less than 5 has been developed by Kee et al. [35]. The reader is referred to reference [35] for further information and some numerical details for computing thermal diffusion coefficients of light molecules.

Once the binary and thermal diffusion coefficients for all species combinations are known, the diffusion velocities of each species can be computed from equation (10). The diffusion velocity is the velocity induced upon each species by all diffusion processes that are present in the flow. The solution of equation (10) requires solving a simultaneous equation system, with the number of equations equivalent to the number of species present for each component of the diffusion velocity. It should be noted that for i species, however, the system of i equations defined by (10) is not linearly independent. One of the equations must be replaced by the constraint $\sum_{i=1}^{n_s} \rho f_i \tilde{V}_i = 0$ to make the system linearly independent. The resulting simultaneous system of equations must then be solved for the diffusion velocities.

The process of solving for the diffusion velocities can be computationally quite expensive. A coupled system of equations must be solved for each of the three components of the diffusion velocity at each computational grid point. This process can require as much time as solving the Navier-Stokes equations for the three components of the convection velocities. Alternately, for hydrogen-air chemistry where large amounts of nitrogen are present, it is sometimes assumed that each species is present as a "trace" in a mixture with N_2 [26]. Then each species is assumed to diffuse only into N_2 with that process defined by its binary diffusion coefficient with N_2. Finally, for engineering calculations, it is often further assumed that the diffusivities of each chemical species present in the flow are the same. Then the diffusion of each species into the remaining species varies only with its respective concentration gradient. The diffusion velocities then decouple, and equation (10) reduces to

$$\tilde{V}_{i,j} = -\frac{D}{f_i}\frac{\partial f_i}{\partial x_j} \tag{30}$$

where $\tilde{V}_{i,j}$ is the diffusion velocity vector of the i th species in the j th coordinate direction (j = [x,y,z]) and D is the binary diffusion coefficient. If the binary diffusion with N_2 is not used, the value of D is determined by chosing an appropriate value of the Schmidt number Sc since $D = \frac{\mu}{\rho Sc}$. The mixture viscosity μ is determined as before from Wilke's law. When the binary diffusion assumption is invoked, it is often further assumed that the mixture

thermal conductivity can be defined by $k = \frac{C_p \mu}{Pr}$ after an appropriate value of the Prandtl number Pr has been chosen.

Turbulent Diffusion Models

While the techniques for defining the molecular diffusion of momentum, heat, and mass are reasonably well established in a supersonic reacting flow, the same statement cannot be made for our ability to describe the turbulent diffusion of these quantities. Work to develop methods for modeling turbulent supersonic combustion is now in its early stages. Conventional approaches have included the use of algebraic eddy viscosity models or differential transport models. Several eddy viscosity models have been used, in particular the Cebeci-Smith model [36] and the Baldwin-Lomax model [37]. The differential transport models include the k/ϵ turbulent kinetic energy model and its variants [38], a modified k/ϵ model that included a supersonic flow compressibility correction [39,41], and a multiple dissipation length scale (k/multiple ϵ) model with a compressibility correction [39,40] that addressed the existence of multiple dissipation length scales that exist in the energy cascade of a turbulent flow. In addition to these differential transport models, the algebraic Reynolds stress models of Rodi [42] and Sindir [43] have also been considered for use in modeling turbulent supersonic reacting flows. A review of all of these models has been given by Sindir [43]. In that review, he also critically compared the models against several nonreacting flow experiments prior to using the models for studying flows with reaction. He concluded that forms of the algebraic Reynolds stress model that he considered produced the best agreement with nonreacting data. He also found that the multiple dissipation length scale model did not offer any advantage over the basic k/ϵ model.

All of the turbulence models described above have a major disadvantage when applied to reacting flow fields. They fail to account for the important coupling between the fluid mechanics and the chemistry. Turbulent fluctuations in the fluid mechanic variables have a direct effect upon the species production rates. The coupling between these two fields

occurs through the Arrhenius rate expression, equation (15), and the law of mass action, equation (18). The Reynolds averaging process applied to the governing equations eliminates the direct effect of temperature and species fluctuations on species production rates. For example, a positive temperature fluctuation would cause a decrease in the size of the exponential argument of the Arrhenius rate expression, with a corresponding increase in the forward kinetic rate of a particular reaction. This would in turn produce an increase in the time rate of change of the products of that reaction. More importantly, if the reaction were at a critical stage, where perhaps a small increase in temperature would cause a reaction to enter an ignition stage, the entire species distribution of the flow field downstream could be changed.

Two promising ways for accounting for the effects of fluid and species fluctuations on chemical reaction would be through probability density functions or direct numerical simulation. The application of the probability density function approach to a reacting flow has been covered by Stephen Pope in a companion chapter in this book and so that subject will not be further addressed in this chapter. Direct numerical simulation offers another attractive approach for modeling a turbulent reacting flow. The method has been used for a several years to accurately model lower speed reacting flows [44,45,46]. With this approach, the Navier-Stokes and species continuity equations are resolved down to the smallest scale features of the flow field. The size of those scales goes inversely with the Reynolds number of the flow field. Clearly then, for the high Reynolds numbers that occur in typical supersonic reacting flows, the smallest scales can become quite small, nessitating a very fine computational grid to resolve the scales. Also, when high speed flow undergoes chemical reaction, additional scales are introduced by the combustion process. Herein lies the principal difficulty of applying direct simulation to a high speed flow. The difficulty is not so much one of numerical algorithms as it is of computer power. Highly accurate numerical algorithms are required, but appropriate high-order finite-difference/volume methods or spectral methods have been developed that satisfy that requirement. The large number

of computational grid points required to resolve the smallest scales in the flow requires large computer storage, and therefore, meaningful calculations can be carried out only on large memory machines. Currently, direct numerical simulations have been made for nonreacting flows with Reynolds numbers up to about 10000 on a Cray 2 computer [47]. Work is proceeding to directly simulate a chemically reacting flow of a similar Reynolds number, and those activities will be discussed with other applications later in this chapter.

As an alternative to direct numerical simulation with its intensive memory requirements, it is possible to model rather than compute the smallest scales. In this approach, termed large eddy simulation, the larger scales above a chosen wavelength are still computed. The smaller scales below the cutoff wavelength are modeled, however, using a subgrid scale model. Large eddy simulation is an attractive alternative because only the larger scale effects are computed, lessening the computer memory requirements for higher Reynolds number flows. Subgrid scale models must be constructed, though, that give an accurate rendering of the physics of small scale phenomena. This is a difficult task. Work is underway to develop subgrid scale models for nonreacting flow, for example the early work of Schumann [48] and later work described by Speziale et al. [49]. Large eddy simulation is an attractive technique for modeling high speed reacting flows. Little has been done so far with this technique, but it warrants serious attention in the future.

Discretization of the Governing Equations

Once the governing equations and required modeling are in hand, the numerical method of choice can be applied to discretize the governing equations in space and time. The numericist has three basic options for discretizing the equations in time. He may express the equations explicitly, implicitly, or in a partially implicit manner. The merits of the first two approaches were discussed in the introduction. The latter approach is attractive when the time scales for chemical reaction are quite small as compared to the prevailing fluid dynamic time scales. In this case, the governing equations become stiff, and a significant

advantage can be gained in convergence of the equations to steady state by casting only the source term in the equations implicitly [50,51]. Before discretization, it is convenient to express the governing equations (1) in vector form. In that form they become,

$$\frac{\partial \vec{U}}{\partial t} + \frac{\partial \vec{E}}{\partial x} + \frac{\partial \vec{F}}{\partial y} + \frac{\partial \vec{G}}{\partial z} = \vec{H} \tag{31}$$

where $\vec{U}$ is the vector of dependent variables, $\vec{E}, \vec{F}$, and $\vec{G}$ are flux vectors continuing convective and diffusive terms, and $\vec{H}$ is the source term containing body forces and the chemistry production terms. The temporally discrete form of equation (31), written explicitly, is then given by

$$\vec{U}^{n+1} = \vec{U}^n - \Delta t[\frac{\partial \vec{E}^n}{\partial x} + \frac{\partial \vec{F}^n}{\partial y} + \frac{\partial \vec{G}^n}{\partial z} - \vec{H}^n] \tag{32}$$

where n is the old time level and n+1 is the new time level. Written implicitly, equation (31) becomes

$$\vec{U}^{n+1} = \vec{U}^n - \Delta t[\frac{\partial \vec{E}^{n+1}}{\partial x} + \frac{\partial \vec{F}^{n+1}}{\partial y} + \frac{\partial \vec{G}^{n+1}}{\partial z} - \vec{H}^{n+1}] \tag{33}$$

A partial implicit statement of equation (31) is obtained when only the source term is written implicitly, i.e. $\vec{H^{n+1}}$, and the remaining terms are written explicitly.

Once the temporal discretization of equation (31) has been chosen, the spatial derivatives must also be discretized. There are many choices available. In the next section of this chapter, we will examine a number of those choices, using earlier techniques as well as some newer ones. We will then be in a position to review some applications of these methods to practical supersonic combustion problems that we are able to numerically simulate today.

Numerical Algorithms

A number of numerical algorithms have been used over the past 20 years to solve the equations that govern a supersonic reacting flow field. The earliest of those approaches were reviewed briefly in the introduction to this chapter. We will now discuss, in somewhat

more detail, several of those algorithms that are still in use today. New algorithms that have appeared fairly recently will then be considered, and their merits and the advantages that they offer over the older approaches will be discussed. Accurate methods used in other fields and recently borrowed to model combustion problems will also be reviewed. With the review behind us, we will then move on in the next section to the application of these algorithms to several practical combustion problems. We will then be in a position to assess where we are in our ability to model these practical combustion problems and what is needed to further extend our capabilities.

Conventional Approaches

The algorithms developed by Spalding, Dash, MacCormack, and their colleagues today continue to be popular tools for modeling supersonic reacting flows typical of those found in scramjet combustors. Each of these algorithms was described in the introduction, and references were given to provide more details. The Spalding three-dimensional parabolized Navier-Stokes code, SHIP [12] as modified by Evans [14], is still being used to carry out engineering design studies of scramjet configurations as well as basic high speed fuel-air mixing studies. The two-dimensional parabolized Navier-Stokes code, SCORCH, of Dash [15] has recently seen considerable use to perform analyses of the National Aero-Space Plane (NASP) propulsion system. In addition, the SCORCH code has also been used to carry out several fundamental studies of experiments being used to design that propulsion system. The MacCormack algorithm was employed by Drummond in the TWODLE code [19,22] to solve the two-dimensional Navier-Stokes equations describing a scramjet flow field. We will examine some interesting computations from these conventional algorithms in the applications section of this chapter.

A number of other extensions of the MacCormack algorithm were made following the work that was just described. Drummond extended the TWODLE code [52] to include detailed models for finite rate chemistry and kinetic theory based models for the molec-

ular diffusion of momentum, heat, and species. He also added an option for treating the chemical source term implicitly, as suggested by Bussing and Murman [50], to allow for a more efficient treatment of stiff kinetic source terms. In that form, the new code (SPARK) then solved in two-dimensions without simplification the complete governing equation set given in equations (1) through (29). Options were also provided, however, to simplify the diffusion modeling to use the approach indicated by equation (30). Following development, the SPARK code was also applied to NASP configurations, but perhaps more importantly, it was also applied to a number of basic high speed reacting flow problems to seek an improved understanding of important physical processes that occur in these flows and that ultimately effect the performance levels that can be achieved by the propulsion system.

As scramjet technology evolved, a critical need developed for a three-dimensional analysis tool for modeling high speed combustor flow fields. Uenishi and Rogers [53] extended the three-dimensional nonreacting Navier-Stokes inlet code (NASCRIN) developed by Kumar [54,55] to include multiple species, but initially they did not include chemical reaction. The program again used the unsplit MacCormack method [16] to integrate the governing equations (1) through (10). Thermodynamic properties were also defined using equation (11) and the procedure described in the discussion following that equation. Molecular diffusion of momentum, energy, and species was modeled with Sutherland's and Wilke's law, the Reynolds analogy, and Fick's law, respectively. Turbulent diffusion was modeled with the Baldwin-Lomax turbulence model [37] along with chosen values of the turbulent Prandtl and Schimdt numbers. A clever storage scheme was also employed with MacCormack's predictor-corrector scheme that saved predictor values locally only until the corrected values could be computed [55]. The scheme allowed computations to be carried out, with three chemical species, on computational grids with up to 500,000 points on a Cyber-205 having 32 million words of storage. When the code was completed, a number of studies were made to model supersonic fuel-air mixing in scramjet like flows [53]. Of particular interest were the calculations of the downstream mixing of a transverse hydrogen

fuel jet injected across a supersonic air flow. These calculations by Uenishi were the first simulations of the three-dimensional near-field fuel injector problem in a scramjet engine. At that time, a clear understanding of the flow field that existed near the fuel injectors was critical to achieving a successful engine design. Work to optimize fuel injector design based on these and other simulations is continuing today.

Uenishi et al. then extended their program to include finite rate chemical reaction [56]. Motivated by the need to model hydrogen-air combustion taking place in a scramjet, they chose a two-step hydrogen-air reaction model developed by Rogers and Chinitz [57]. The model considered five species (H_2, O_2, OH, H_2O, and N_2 [inert]) participating in the following chemical reactions.

$$H_2 + O_2 \rightleftharpoons 2OH \tag{34}$$
$$H_2 + 2OH \rightleftharpoons 2H_2O$$

The approach defined by equations (15) through (20) was then used with the chemistry model to determine values of the chemistry source terms. The source terms were sometimes found to be numerically quite stiff, and so the numerical method was also modified to include implicit source terms. Otherwise, the numerical method and the physical modeling remained unchanged from the previous code. Uenishi again applied his extended program to the transverse fuel jet problem, but in this case with chemical reaction. Encouraged by those results, he then went on to model an actual combustor configuration. Some results from those calculations will be included in the next section of this chapter.

Because of the need for a more basic modeling capability in three dimensions, Carpenter then extended the SPARK combustion code to three dimensions [59]. The three-dimensional code retained all of the basic modeling of the two-dimensional code, i.e. it solved the system defined by equations (1) through (30). In addition, Carpenter added a generalized equilibrium chemistry model and a generalized finite rate chemistry model that allowed for consideration of any fuel-air system with any number of reaction paths

[60]. Typically, either a seven species, eight reaction model or a nine species, eighteen reaction model was used to represent hydrogen-air chemistry. The eighteen reaction model is given in Table 1. Turbulence was modeled with either a Cebeci-Smith or Baldwin-Lomax eddy viscosity model, or a two-equation k/ϵ turbulent kinetic energy model. Calculations were then carried out to validate the code by modeling several of the problems considered by Uenishi. Following successful agreement with Uenishi's results and experimental data, the code was also used to study a model scramjet combustor. Those results will also be presented in the applications section.

Three-dimensional parabolized Navier-Stokes programs were also developed to model supersonic combustor flow fields. These programs often provided a more efficient solution procedure if the flow field contained no subsonic regions. The flow field in the neighborhood of the fuel injectors in a scramjet combustor contains subsonic separated regions necessitating a solution of the full (spatially elliptic) Navier-Stokes equations. Somewhat downstream of this region, however, the flow takes on a principal supersonic flow direction, allowing solution of the parabolized equations and the application of parabolized codes. In response to this need, Chitsomboon developed a three-dimensional parabolized Navier-Stokes (PNS) program [61] by extending a two dimensional PNS program that he had developed earlier [62,63]. He solved the conventional parabolized Navier-Stokes equations together with a set of species continuity equations given vectorally by

$$\frac{\partial \vec{E}}{\partial x} + \frac{\partial \vec{F}}{\partial y} + \frac{\partial \vec{G}}{\partial z} = \vec{H} \tag{35}$$

where E, F, G, and H have the same definitions as given in equation (31). The dependent variable vector $q = [\rho, \rho u, \rho v, \rho w, T, \rho_i, ...]$ was chosen nonconventionally, with the energy equation written in terms of temperature rather than total enthalpy or total internal energy. The equations (35) were then discretized using the Vigneron method [64], and the nonlinear vectors F, G, and H were linearized with respect to the dependent variable vector q. In order to insure that the numerical scheme was then stable, the flux vector E was linearized using the approach of Schiff and Steger [65]. Thermodynamics and chemistry

were handled in a manner identical to the approach used in the Uenishi code [58]. Following initial completion of the code, it was compared against the Uenishi program and fairly good agreement was achieved. The code is undergoing further development today.

During this same period, Gielda developed a three-dimensional explicit PNS program [66] using the MacCormack explicit algorithm [16]. The code was fully vectorized to run efficiently on vector supercomputers such as the Cray 2 and the Cyber 205. Gielda found that his explicit scheme was quite competitive with implicit algorithms for problems at high Mach number or with surface discontinuities. He was able to resolve the problem of decoding the axial flux vector (E in equation (35)), that had earlier limited the application of explicit PNS codes, by also employing the Vigneron procedure of splitting the axial pressure gradient. Following completion of this nonreacting program, Gielda extended his code (then named the SSCPNS code) by adding the parabolized species continuity equations to the governing equation system [67]. He also incorporated both an equilibrium and a global one-step H_2-air finite rate scheme into the program. The extended program was then validated against several experimental cases, and generally excellent agreement was obtained between data and computation. With this confidence in hand, the code was applied to a three-dimensional generic inlet-combustor scramjet configuration that included gaseous hydrogen fuel injection and reaction. Some of these interesting results will be presented in the following section.

Kamath then employed the Gielda algorithm to develop a parabolized version of the three-dimensional SPARK combustion code [59]. He generalized the coordinate transformation to allow the streamwise coordinate to be orientated in the most supersonic direction. He also utilized the generalized equilibrium and finite rate chemistry schemes developed by Carpenter [60] such that any multistep reaction scheme could be considered with the algorithm. The extended code was next validated with several test cases, one of which was also utilized by Gielda, and it gave generally good agreement with data. Work on the program is now continuing.

Alternate Approaches

Several numerical algorithms have been developed to solve the equations governing high speed reacting flow fields, but these algorithms have not been applied to the scramjet combustor problem. Most of these methods have been developed to model supersonic or hypersonic flow with interacting air chemistry moving externally about configurations. The remaining algorithms have been developed to study basic phenomena associated with high speed reacting flows, but have not yet been applied to scramjet problems. Each of the approaches falls into the general class of monotone methods, that is methods that employ flux-correcting or flux-limiting procedures to preserve high numerical resolution without the numerical oscillations associated with higher accuracy. Included in this class of algorithms are Flux Corrected Transport methods, TVD (total variation diminishing) methods, and TVD like methods that exhibit TVD behavior. These algorithms would offer the modeler advantages over conventional methods when studying scramjet problems, and they should be seriously considered for future work. It is for that reason that we discuss them here.

The first monotone method applied to chemically reacting flows was the Flux Corrected Transport (FCT) algorithm developed by Boris [68,69,70]. In this method, a small amount of artificial diffusion is added to the governing equations in smooth regions of the flow to stabilize the solution. In regions where high gradients exist, larger amounts of diffusion are added to maintain monotonicity. The diffusion is added in such a manner, however, that the overall dissipation is held below that of the conventional algorithms. One proceeds as follows. Starting with equation (32), the flux terms are discretized in space, and then a diffusive term is added to insure positivity as the equations are integrated in time. That integration is then performed to determine a first value of the dependent variable vector at the next time step. An "anti-diffusive" correction using the first values of the dependent variables is then applied to reduce the numerical diffusion added in the first step. Care must be taken when applying this step, however, because the anti-diffusive correction can

degrade the monotonicity of the method. Therefore, the anti-diffusive terms are limited by a "flux correction" procedure such that no new maxima or minima are introduced into the solution. The initial fluxes in equation (32) are then replaced by the corrected fluxes and the equation is again advanced over the same time step to arrive at the final value of the dependent variables at the new time. A more detailed but very readable description of the FCT method is given in reference [70].

Following development of the FCT method, a more general approach was suggested by Zalesak [71]. His approach allowed the method to be readily incorporated into existing algorithms that did not provide monotone behavior. In addition, the method could be more easily generalized to two and three spatial dimensions. Zalesak viewed FCT as a hybridization of a low order and a high order method. The anti-diffusive flux was then found as the difference between the fluxes determined by the high order and low order methods. Once found, the anti-diffusive flux was then limited as before by flux correction, and the solution was advanced using the corrected fluxes. A more detailed discussion of Zalesak's approach is again given in reference [70].

Most of the new work to model high speed reacting flows has taken place over the last five years. It was motivated primarily by the need to model hypersonic flows about vehicles, including hypersonic cruise aircraft such as the NASP, and reentry vehicles. Therefore, the methods were developed to model high speed strongly shocked flows undergoing air chemistry. To compute flows of this type, MacCormack and Candler developed an implicit flux split scheme, as an extension to MacCormack's explicit predictor-corrector finite difference method [16], to solve the Navier-Stokes equations. MacCormack initially developed the implicit algorithm to consider only nonreacting flows [72]. A finite volume approach was used to discretize the flux terms. In addition, Steger-Warming [73] flux vector splitting was introduced to more properly account for the propagation of information through the flow field. Finally, to relax the constraint on the time step imposed by the Courant condition in his explicit method, the flux terms were written implicitly and then linearized.

This procedure resulted in a coupled set of algebraic equations to be solved at each time step once the spatial opperators had been applied to the flux terms. The equation system was then solved iteratively using either a line Gauss-Seidel procedure or Newton iteration.

Following development of the basic algorithm, Candler and MacCormack extended the method to consider high speed air flows that were ionized and in thermodynamic and chemical nonequilibrium [74,75]. To model such flows, equations describing species continuity, vibrational energy of each diatomic molecule, and electron energy were appended to the Navier-Stokes equations. The fully coupled system of equations was again solved using Gauss-Seidel line relaxation along with an implicit, flux split treatment of the flux terms. Air chemistry was modeled with a seven species, six reaction model that included $N_2, O_2, NO, NO^+, N, O,$ and e^-. For these species, four vibrational temperatures and an electron temperature were computed. The chemical source terms associated with the seven species and the thermal source terms were also computed implicitly due to the small kinetic time scales, relative to fluid scales, that were introduced by the chemistry. When the authors completed the extension of their algorithm to include chemical reaction, they applied it to several high speed external flow problems in both two- and three-dimensions that are described in references [74] and [75]. Even though these examples considered only external flows with air chemistry, it appeared that the algorithm could readily be modified to consider internal flows with combustion chemistry, and, therefore, serve as a means for modeling scramjet combustor flow fields.

Flux splitting methods were also employed by Grossman, Walters, and Cinnella to model high speed chemically reacting flow problems. Grossman and Walters initially developed their algorithm to solve the Euler equations for nonreacting flows, but included real gas effects [76]. Three forms of flux splitting were considered, including Steger-Warming flux vector splitting [73], van Leer flux vector splitting [77], and Roe flux difference splitting [78]. Each of these splitting methods was originally derived to be applied to ideal gas flows. They were rederived in reference [76] to allow their application in problems

with real gas effects. The new derivations are based on the concept of an equivalent γ to replace the ratio of specific heats for an ideal gas. Each approach is derived with sufficient detail in the paper to allow the reader to incorporate the modifications into existing flux split codes written to originally model ideal gas flows. Once the flux split equations had been developed, they were solved using a two-step predictor-corrector method that was second-order accurate in space and time. Spatial differences were formed using the MUSCL differencing procedure and flux limiting that was described in reference [79]. Following the successful application of the algorithm to a one-dimensional shock tube problem, the real gas splitting was incorporated into a two-dimensional implicit finite volume code that originally utilized van Leer splitting and Gauss-Seidel line relaxation to solve the equations governing ideal gas flows [80]. The modified code was then applied to a two-dimensional inlet flow field exhibiting equilibrium real gas behavior.

Grossman and Cinnella then extended the algorithm to include vibrational and chemical nonequilibrium [81,82]. They again began with the one-dimensional Euler equations, but they appended species continuity equations to account for each chemical species present in the reacting flow and vibrational energy conservation equations to account for those species in vibrational nonequilibrium. The authors then redeveloped the relationships described previously that were required to implement Steger-Warming, van Leer, and Roe flux splitting. Once these splitting approaches had been implemented, a finite volume scheme was used along with either an explicit Runge-Kutta time integration or an implicit Euler time integration to solve the governing equations. The shock tube problem was again revisited, but nonequilibrium effects were modeled with a five species, five reaction model that included $N_2, O_2, NO, N,$ and O. Finally, a supersonic nozzle flow undergoing H_2-air chemistry was modeled using a five species, two reaction model involving $H_2, O_2, OH, H_2O,$ and N_2. The calculations exhibited excellent agreement with those provided by another program utilizing a conventional method [81]. Extensions of the algorithm to two- and three-dimensions are currently underway, and once in place, this approach should also offer

an attractive option for modeling scramjet combustor flow fields.

A class of more exact flux split algorithms for nonequilibrium chemistry was recently developed by Liu and Vinokur [83]. Steger-Warming, van Leer, and Roe flux splitting were again generalized for the nonequilibrium case. No simplifying assumptions were made, however. The most general thermal and chemical nonequilibrium flow of an arbitrary gas was considered. The results have not yet been incorporated into a computer program, but one should become available in the future.

Additional interesting work using flux splitting has also recently been completed by Liou, van Leer, and Shuen [84]. This work has only recently been submitted for publication and so details will not be given here. The authors again employed van Leer flux vector splitting or Roe flux difference splitting and derived real gas forms of these approaches. The derivations were begun by assuming a general equation of state for a real gas in equilibrium. Approaches similar to those discussed previously were then used to modify the splittings, but the number of assumptions and particularizations employed were kept to a minimum. The modified splittings were then incorporated into an available TVD algorithm [85] and used to model several problems described by the one-dimensional Euler equations. Excellent agreement with the exact solution for a classical shock tube problem was obtained [84]. Work on the method is now continuing.

A considerable amount of work has also been carried out over the last several years to develop new TVD schemes for chemically reacting real gas flows. Beginning in 1985, Yee developed a symmetric TVD scheme that could be employed in the context of either explicit or implicit numerical integration procedures [86]. The approach was later generalized to consider chemically reacting flows [87]. Yee noted that her approach could readily be added to existing algorithms that did not exhibit TVD behavior, e.g. the 1969 MacCormack method, resulting in a more robust method with better shock capturing qualities. New explicit, semi-implicit, and implicit algorithms employing the symmetric TVD method were then developed and discussed [87]. An explicit multistep TVD scheme

was constructed using the 1969 MacCormack method [16] for the first two (predictor-corrector) steps followed by the addition of a conservative dissipation term as a third step, such that the overall scheme was TVD. The dissipative term was made up of products of eigenvectors of Jacobians of the governing equation system and their associated eigenvalues, an entropy correction, and a limiter function. Details regarding the construction of the dissipative term and the determination of its magnitude were given in reference [88]. For the situation described earlier, where stiff kinetics resulted in small chemistry time scales, the explicit procedure was altered to include an implicit source term while retaining explicit flux derivatives and the same dissipative terms. Finally, a fully implicit TVD method was developed that included both implicit source and flux terms for situations where both chemistry and fluid scales were small. Calculations using both the explicit and semi-implicit schemes were also given in reference [87]. The explicit scheme was used to model a shock interacting with an obstacle in a two-dimensional flow. The shock was captured quite crisply, and more subtle flow discontinuities, including slipstreams that were present, were also captured. The semi-implicit scheme was generalized to three-dimensions and incorporated into the Uenishi semi-implicit code [56] that was described earlier in this chapter [89]. That program also contained the two step Rogers-Chinitz H_2-air chemistry model discussed before. The three-dimensional TVD code was then used to model the reaction of a stoichiometric H_2-air mixture flowing supersonically in a channel [89]. The flow was ignited by a shock produced by a wedge along the lower wall of the channel. The resulting fluid and chemistry profiles predicted by the program in the neighborhood of the shock did not exhibit the overshoots and undershoots typical of those observed with classical shock capturing methods.

When stiff terms are present in the governing equation system and the fully implicit TVD procedure of [87] is used to solve two- or three-dimensional problems, the procedure employed to temporally integrate the governing equations must be carefully chosen. When ADI procedures are used, the factorization error that results when the implicit

operator is spatially factored often cannot be neglected [87]. Iterative procedures such as line Gauss-Seidel or Newton iteration, applied in the approaches discussed earlier, are attractive options. An alternate procedure developed by Gnoffo employed point implicit relaxation [90,91]. That procedure was used by Gnoffo in his three-dimensional finite volume code that employed a symmetric TVD upwind discretization of the governing Navier-Stokes, species continuity, vibrational, and electron energy equations. Pseudo-time relaxation was used to drive the solution to a steady state. A point-implicit procedure implies that during a relaxation step, the equations at each cell in the computational plane are discretized by using the latest available data from neighbor cells and by implicitly updating only those terms which are functions of variables at the cell center. This procedure has proven to be very efficient on vector computers. Two options for coupling the governing fluid and chemistry equations, strong and weak implicit coupling, were also utilized. With strong implicit coupling, the complete equation set was solved as a unit, an approach typical of those described earlier. Weak implicit coupling involved splitting the fluid and chemistry equations into two groups, and applying the point-implicit method to each group separately during the relaxation process. The former approach was more physically exact, better accounting for complex wave interactions and fluid-kinetic coupling. The latter approach allowed for the relaxation strategy and time stepping to be tailored to the needs of the equation set [91]. Air chemistry was modeled in the program using an eleven species scheme that included $N, O, N_2, O_2, NO, N^+, O^+, N_2^+, O_2^+, NO^+$, and e^-. Further details on the chemistry model and other physical modeling are given in reference [92]. Gnoffo's program was validated against several experiments and has performed well. The code was then used to successfully model the high speed external flow about several configurations. Because of the code structure, it should be relatively straightforward to add a H_2-air combustion model. Therefore, Gnoffo's program, utilizing a symmetric TVD upwind discretization with point-relaxation appears to be an attractive candidate for modeling scramjet combustor flow fields as well.

Another attractive option to an ADI integration scheme for solving the spatially discretized governing equations is an LU scheme that approximately splits the implicit operator into an upper and a lower operator which is independent of the dimensionality of the problem. Shuen and Yoon developed a scheme for solving the two-dimensional Navier-Stokes and species continuity equations governing chemically reacting flows that employed an implicit finite volume time marching LU method [93]. Details of the derivation of the LU scheme are given in the reference. The approach was quite attractive because, even though the method was fully implicit, it required only scalar diagonal inversion for solution of the flow equations and diagonal block inversion of the species equations. The authors stated that as a result, the scheme exhibited a fast convergence rate while requiring only about the same amount of work as that of an explicit method [93]. This advantage can be particularly important when problems with a large number of chemical species are being solved. Following development of the LU code RPLUS, an eight species, fourteen reaction chemistry model and the Baldwin-Lomax algebraic turbulence model was added to the program. The code was then compared with experimental data and calculations from other combustion programs, and it showed very good agreement with those data and computations [93]. Encouraged by their success, Yu and Shuen then extended the LU code to three-dimensions (RPLUS3D) [94]. A finite rate chemistry model and a turbulence model are currently being added to the program. Once completed, the three-dimensional LU code will provide another valuable tool for modeling scramjet combustor flow fields.

The alternative methods described above for modeling reacting flows (with the exception of Flux Corrected Transport) have generally exhibited second-order numerical accuracy in both space and time. Two high-order accurate methods have recently been developed and applied to high speed combustion problems. These methods offer improved accuracy as compared to lower-order methods on a given computational grid and reduced phase error. One method was developed by Carpenter using a fourth-order compact finite difference scheme [59]. The scheme was initially developed by Abarbanel to accu-

rately solve the Euler equations in two- and three-dimensions [95]. Carpenter extended these ideas to the Navier-Stokes equations and used them to alter the 1969 MacCormack method, producing a fourth-order "compact MacCormack" scheme. The modifications did not change the basic structure of the MacCormack scheme, allowing it to be easily incorporated into existing codes using the 1969 algorithm. The modification significantly improved the accuracy of the algorithm, while markedly reducing the phase error. As a result, the improved scheme was able to crisply capture strong shocks with very little of the pre- and post-shock oscillations present in the old scheme. The algorithm in fact exhibited a TVD like behavior when capturing waves. Because of its attractiveness, the scheme was added to the two- and three-dimensional SPARK codes and applied to several supersonic chemically reacting flow problems [59]. Very good agreement with available experimental data was achieved, and the 3-D program was then successfully applied to a three-dimensional scramjet combustor. Results from that study will be described later in this chapter.

High-order accurate spectral methods have also been applied to supersonic reacting flows. Drummond extended a Chebyshev spectral method developed to study transitioning flows [96,97] to include finite rate chemical reactions [98]. Spectral methods are based on the representation of the solution of a problem by a finite series of global functions, in this case Chebyshev polynomials. To apply this method to the Navier-Stokes and species continuity equations, the flux terms in these equations were restated in terms of Chebyshev series, and then the required spatial derivatives were taken. The resulting ordinary differential equations were then integrated with respect to time using a Runge-Kutta time stepping scheme. Drummond initially developed this technique for the one-dimensional Euler equations and species continuity equations [98]. The method was then extended to two-dimensions in reference [99] where a hybrid spectral-finite difference algorithm was used to model two-dimensional supersonic reacting flows.

Now that both conventional and new alternate methods for modeling supersonic react-

ing flows have been examined, we will now explore the results from some of the problems where these methods have been applied. This should make more clear how far we have been able to carry these techniques to solve some of the difficult problems that we face in the course of designing and developing a scramjet engine.

Applications

Many of the computer programs described earlier in this chapter have been applied to study supersonic reacting flow fields. In this section, we will review some of those applications. Space does not allow a review of each effort. Rather, a representative sample of the research will be provided to show the progress that has been made. We will begin with some basic two-dimensional studies performed in the late 1970's. We will then examine some of the first attempts to model simple scramjet flow fields and see how those studies affected later design activities. The early scramjet studies raised several basic issues regarding mechanisms controlling the mixing and chemical reaction of fuels and air at supersonic speeds. These issues spawned several research efforts undertaken to better understand high-speed combustion physics and to use that understanding to improve engine performance. Therefore, we will next examine the results of some of those efforts. With advancing computer resources in the mid 1980's, scramjet calculations moved ahead to consider three-dimensional reacting flows. Those calculations began with simple three-dimensional configurations that served as model problems for the more complicated configurations to be later considered. We will complete our review of the applications by tracking the progress of those three-dimensional calculations, ending with a complex combustor configuration not greatly different from those being considered for advanced propulsion systems to be employed early in the next century.

Early supersonic reacting flow simulations centered on configurations defined by experiments that were being performed at that time. Evans, Schexnayder, and Beach used the CHARNAL program as modified by Evans [14] to model a number of experiments

available in the late 1970's and compared their simulations with the available data [100]. One case, the Burrows and Kurkov experiment [101], is shown in figure 1. Hydrogen was injected at Mach 1.0 through a slot in the lower wall of the configuration. Hot air passed by the slot at Mach 2.44. The air temperature was sufficient to ignite the hydrogen gas. Figure 2 shows a comparison between the computed results and the data including pitot pressure and reactant and product mass flow 35.6 cm downstream of the slot. The calculations were made using either a complete (infinitely fast) or a finite rate (eddy breakup) model [100]. The agreement between the data and calculation is quite good for both pitot pressure and chemical species distributions. Encouraged by their success, the authors went on to examine several other experimental cases, each of which is discussed in reference [100].

While basic combustion studies continued, some of the effort was shifted to begin considering scramjet combustor flow fields. The first efforts considered only a part of the combustor, and they were still limited to two-dimensions. One example is given in figure 3 which shows a sketch of a slot injection experiment undertaken to simulate the transverse injection of fuel into a scramjet combustor. In this case, helium was injected at Mach 1.0 into a Mach 2.9 air cross-stream in a duct. Helium was used to represent gaseous hydrogen fuel because the test facility in which the experiment was performed could not support combustion. Weidner and Drummond modeled the flow field in the channel using the TWODLE code [22] and obtained the results shown in figure 3 [23]. Comparisons of the calculations with measured static pressures were fair and the comparison with helium mass fraction was quite good. (Interest in the slot injector case continued through the 1980's. Shuen and Yoon revisited this case in 1988 using their new LU scheme in the RPLUS code and showed improved agreement with the static pressure data [93]. They also went on to examine a reacting hydrogen-air transverse jet case and reported those results in that reference.) Following the nonreacting study, Weidner and Drummond went on to consider several two-dimensional transverse injector configurations including the "staged" injector

configuration shown in figure 4 [23]. Staged injection of hydrogen fuel provided a means for producing a large region of separated flow between the injectors, thereby providing improved flameholding in the combustor. The final configuration resulting from the study is shown in figure 5. A large region of separation was produced between the injectors and significant reaction of hydrogen fuel and air took place in that region.

Following completion of the fuel injector studies, scramjet calculations were extended in 1981 to consider a model problem for a complete engine module including both inlet and combustor. The calculations were still constrained to two-dimensions due to available computer resources at that time. Drummond and Weidner used the TWODLE program to simulate the flow through the module shown in figure 6 [22]. The left portion of the module provided inlet compression and the combustor made up the right portion of the module. A single fuel injection strut was positioned between the two module walls. Gaseous hydrogen fuel (indicated by the arrows) was injected at Mach 1.1 from the strut walls as well as from the engine side walls. That fuel reacted with air that entered the inlet at Mach 5.0. The resulting velocity, static pressure and temperature contours, and water contours are also shown in figure 6. The air entering the inlet was turned by shocks from the inlet leading edges. Shocks are indicated by a coalescence of pressure contour lines in the figure. These shocks struck near the strut leading edge and coalesced with shocks produced by the strut. The resulting shocks then had sufficient strength to separate the boundary layer when they reached the engine sidewalls, as indicated by a reversal of the velocity vectors.

The transverse hydrogen fuel injectors located downstream of the minimum can also be seen in the figures along with their associated flow separations leading and trailing the injectors. The flow becomes subsonic near the fuel injectors due to air flow blockage and heat release from chemical reaction. Some reaction takes place in the separated regions ahead of the injectors. Significant reaction occurs downstream of the injectors. The temperature rise and water production associated with the reaction can also be seen in the figures. The

results of the simulation show that the injectors are not of sufficient strength to penetrate across the flow at the point of injection. The mixing layers do not meet until around 11 cm downstream of the injectors. In an attempt to improve the level of fuel-air mixing, the injectors were moved a small distance upstream of their previous location. It was hoped that the change would improve the amount of injector interaction and enhance mixing. The resulting velocity field is shown in figure 7. An inlet-combustor interaction and choking then occured, resulting in large regions of separated flow in the inlet, and clearly, an unacceptable design. To examine the source of choking, the calculation was repeated without chemical reaction. The calculation then proceeded normally without any significant separation. Therefore, it was concluded that thermal choking produced by chemical reaction and subsequent heat release near the injectors produced the inlet-combustor interation. While performed for a two-dimensional engine model problem, these scramjet simulations did demonstrate in 1981 the potential of numerical modeling for studying and better understanding engine flow fields. As computer resources improved, calculations of this type in three-dimensions were also attempted. The calculations also raised some basic questions regarding the very complex physics of mixing and reaction at supersonic speeds in a scramjet combustor. These questions resulted in several research efforts aimed at achieving an improved understanding of these phenomena. We will now move on to describe some of those basic studies and then complete this section by examining some three-dimensional simulations of scramjet combustor flow fields.

The supersonic velocities that must exist in a scramjet combustor produce a perplexing, but interesting problem for the engine designer. At such high speeds, the mixing of the hydrogen fuel injected into the combustor and air from the inlet is reduced relative to the mixing achieved in lower speed operation. As a consequence of the reduced mixing, the degree of reaction that can occur and the overall combustor efficiency is also suppressed. The phenomena of reduced mixing in nonreacting mixing layer flows at supersonic speeds had been observed experimentally by Brown and Roshko as early as 1974 [102], and the

effect was further studied by Papamoschou and Roshko [103] in 1986. Numerical studies of the nonreacting problem by Oh in 1974 [104] and Hussaini, Collier, and Bushnell in 1986 [105] were performed to better understand this phenomena. Oh suggested that the reduced mixing was related to weak shocks that formed when the local Mach number exceeded one about vortical structures that developed in an evolving mixing layer. He argued that other vortices would then interact with these shocks and produce fluctuations in the flow field that could ultimately reduce the turbulent kinetic energy and the degree of mixing. Hussaini et al. examined the detailed interaction of a vortex convecting subsonically relative to a locally supersonic flow. They showed that a transient shock structure which they termed an "eddy shocklet" formed as the eddy accelerated, and the shocklet tended to deform the eddy. Finally, do to this interation, a vortex of opposite circulation formed, and the length scale of the original vortex was reduced. Based on those results, the authors then concluded that eddy shocklets reduced turbulent mixing through both the production of counter fluctuating vorticity and a reduction of turbulence scale.

The effects of chemical reaction on mixing in a supersonic flow have also been considered. Beginning in 1986, Drummond studied the supersonic reacting mixing layer that formed between coflowing streams of hydrogen gas and air at moderate Mach numbers in the range of Mach 2 [52,99,106]. His simulations using the SPARK code indicated that supersonic reacting flows exhibited some of the same features observed for subsonic reacting and nonreacting flows. Vortical structure, noted in much of the subsonic nonreacting flow literature, was shown to be quite predominant. In agreement with the earlier reacting subsonic literature, the vortical structure had a marked effect on chemical reaction in supersonic flow. Significant burning took palce in the eddies on the edges of the mixing layer, broadening the reaction zone relative to the layer thickness defined by the velocity gradient. In addition, the vortical flow resulted in the roll up of unburned reactants inside a layer of partially or fully burned products. This phenomena, often termed "unmixedness" in subsonic flows, prohibited the reaction of captured reactants and reduced the overall

efficiency of the combustion process. There was also some indication that heat release resulting from the chemical reaction also reduced the amount of mixing and reaction further downstream in a mixing layer.

Work is continuing to better understand the phenomena that produce reduced combustion efficiency in supersonic combustors. Related efforts also began in 1987 to develop techniques for enhancing the degree of fuel-air mixing and combustion that occured in high Mach number flows. Guirguis used the flux-corrected transport algorithm of Boris to study convective mixing in high-speed nonreacting flows [108]. He again chose the mixing layer as a model problem for mixing in a scramjet combustor and solved the two-dimensional Euler equations to examine the effects of imposed pressure gradients on the spatial development of the layer. The upper stream of the mixing layer, made up of "species 1" entered a confined channel at Mach 4.5 and a pressure of 4 atm. The lower stream of "species 2" entered at Mach 1.5 and a pressure of 2 atm. The stream temperatures were matched. In addition, two other cases were considered. In the second case, the pressures of the two streams were matched and the mixing layer was unconfined, and in the third case, the lower stream entered at a pressure of 2.1 times that of the upper stream. Other minor differences between the cases were discussed in reference [108]. One result from the study by Guirguis is shown in figure 8. In that figure, mass fraction contours of species 1 from 0.01 to 0.99 are plotted for the three cases, respectively. The matched pressure case showed little development with increasing streamwise coordinate, whereas the first and third cases with the imposed transverse gradient showed significant spread of the layer. Guirguis therefore concluded that in a channel of a given length, differences in pressure across the layer enhanced mixing. He also suggested means whereby pressure differences could be induced by the geometry of the combustor. Guirguis then continued his work to find a means of enhancing mixing where the two stream pressures were matched [109]. He concluded that mixing could be enhanced if a bluff body was placed at the trailing edge of the splitter plate separating the two matched pressure streams. One result from the bluff

body case is shown in figure 9. The mass fraction contours given in the figure again show a significant degree of enhancement is provided by the presence of the bluff body.

Kumar, Bushnell, and Hussaini also examined the problem of mixing in flows undergoing supersonic combustion using a two dimensional version of the NASCRIN Code [110]. Several techniques for enhancing turbulence and mixing were suggested and one enhancement technique that employed an oscillating shock was studied numerically. In this case a premixed stoichiometric hydrogen-air flow was processed through a spatially and temporally oscillating shock wave, and the resulting flow was studied with and without chemical reaction. Reaction was modeled using an equilibrium chemistry model. One reacting flow case that was considered is shown schematically in figure 10. Here, the premixed fuel-air flow was introduced into a two-dimensional channel at Mach 3, a pressure of 1 atm, and a temperature of 1500 K, and the mixture was passed through a 10 degree shock produced by a lower wall compression. A periodic oscillation was imposed upon the flow near the lower wall, and this resulted in a periodic oscillation of the shock wave. The resulting pressure field over one period of the imposed oscillation is shown in figure 11. A wave can be seen to propagate along the shock. The oscillating shock was shown to increase the level of turbulence in the flow field, and the degree of turbulence enhancement was seen to increase with a decreasing frequency of shock oscillation. Chemical reaction as defined by the equilibrium model was shown to have little effect relative to the nonreacting results.

Several techniques for enhancing mixing and reaction in a model scramjet combustor were studied in 1988 by Drummond and Mukunda [107]. They considered the shock and expansion structure that existed in scramjet combustors, and sought to redirect this existing wave structure to utilize it for enhancement. Planar and curved shocks were created by structure and fuel injection in scramjet engines, and so both shock shapes were considered as candidates for mixing enhancement. Three cases that were studied to determine the efficiency of shock shapes are shown in figure 12. Case 1 shows a two-dimensional spatially developing supersonic mixing layer that served as a baseline to indicate the degree of mix-

ing and reaction that could be achieved without enhancement. Here, gaseous hydrogen fuel and air are initially separated by a thin splitter plate. Hydrogen and air both enter at Mach 2, a pressure of 1 atm, and a temperature of 2000 K. The hydrogen and air begin mixing at the trailing edge of the splitter plate, ignition occurs at some small distance downstream, and combustion continues from that point. Two enhancement studies, cases 2 and 3, are also shown in figure 12. In case 2, the mixing layer is processed through two 10 degree planar shocks produced by wedges in the fuel and air streams. In case 3, a small interference body that produces a curved bow shock is placed at the center of the mixing layer. The flow field in each case was then simulated using the SPARK code. Chemistry was modeled using either a 4 species, 1 reaction or a 9 species, 18 reaction H_2-air finite-rate chemistry model. The resulting instantaneous mixing efficiencies shown as a function of streamwise coordinate are given in figure 13 [107]. The degree of mixing achieved in the mixing layer without enhancement is shown by the result from case 1. Very little additional mixing results from passing the layer through planar shocks in case 2. Case 3 exhibits a significantly higher degree of mixing. When the high velocity gradient across the mixing layer is processed by the curved bow shock, vorticity is produced, and the mixing is subsequently enhanced downstream of the shock.

With a background of planar and curved shock mixing enhancement in hand, fuel injection configurations typical of those used in a scramjet engine were considered. A typical design is described in figure 14, which shows the trailing edge of a NASA Langley fuel injection strut. Inlet air crossed the strut as shown. Gaseous hydrogen fuel was injected parallel to inlet air from the base of the strut, and transverse to the inlet air behind a small rearward facing step in the surface of the strut. (The step caused a small recirculation region to form which captured a small amount of fuel and air. Combustion then occured in that region providing a flameholding sight in the engine combustor.) The results of the previous analysis suggested a simple change in the fuel injector configuration that might provide improved fuel-air mixing and enhanced combustion efficiency. If the

parallel injector from the strut base were moved to the step face as shown in figure 14, then the high velocity gradient of that jet would interact with the curved bow shock that formed ahead of the transverse injector. The mixing enhancement modification was then examined by again simulating the two-dimensional flow fields. Chemical reaction was described by the 9 species, 18 reaction finite rate model. The resulting water mass fraction contours downstream of the modified strut for only the parallel injector and for both the parallel and transverse injector are given in figure 14. The multiple jet configuration clearly gave significantly higher levels of jet development, mixing, and reaction. A quantitative assessment of mixing and reaction is given in figure 15. In that figure, the combustion efficiency for both cases is plotted against the streamwise coordinate. Jet interaction produced a significantly more rapid increase in mixing and combustion. Instantaneous combustion efficiencies of about 80 percent were obtained for the enhanced case within the first 40 percent of the solution length whereas the unenhanced case required about 75 percent of the solution length to achieve the same level of reaction. Enhancement by such approaches could therefore result shorter combustor lengths for a given level of performance.

While the basic studies we have discussed were underway, several interesting three-dimensional scramjet combustor simulations were undertaken in 1987 and 1988. Uenishi, Rogers, and Northam used their three-dimensional combustor code, described earlier, to study several generic combustor configurations that utilized wall fuel injection [56,58]. One of the interesting cases is shown in figure 16. This combustor model was also being used in an experimental program at NASA Langley when the study was undertaken, although no data was yet available. Vitiated hot air, produced by the combustion of hydrogen, oxygen, and air in a facility heater, entered the model combustor from the left. Gaseous hydrogen fuel was initially injected a small distance downstream from this point through a row of secondary orifice fuel injectors located on opposite walls of the combustor. These injectors were intended to pilot a pair of primary hydrogen fuel injectors again located on opposite

walls some distance downstream of rearward facing steps in the walls. The flow in the combustor was modeled using the Uenishi code [58]. Features of the combustor flow field resulting from that study are shown in figure 17. Figure 17a shows the distribution of the injected fuel given as the mass fraction of total H_2 in the streamwise x-z plane of the computation along the duct centerline. The total H_2 distribution represented the sum at each point of the hydrogen atoms in any form, i.e. H_2, H_2O, or OH, so that it represented the amount of injected H_2 fuel. The fuel rich regions in the vicinity of the injectors are clearly evident as is the penetration of the fuel across the duct. The contours in figure 17a show that the upstream fuel injectors provide relatively well mixed fuel and air into the downstream region which then arguments the fuel mixing and combustion process produced by the downstream injectors [58].

The three-dimensionality of the flow field is clearly shown by the distributions of total H_2 and static temperature given in figure 17b at several cross-planes along the combustor length. The static temperature was normalized by the initial static temperature. The locations of the y-z cross-planes are indicated in figure 17a. The distribution of total H_2 in each cross-plane indicates the mixing of injected fuel. At location A, the fuel jets from the upstream injectors have not merged, and the cold fuel has not mixed with the hot air stream to an extent sufficient to result in any significant heat release, as is indicated by the absence of any appreciable temperature rise at this location. At location B, however, the fuel has mixed and reacted with the hot-air stream to an extent that the temperature is about 1.7 times the air stream. Further downstream, at locations C and D, the 0.5 percent contour line becomes more uniform and a large area of the flow contains reacting fuel as also indicated by the elevated temperatures. Results from location E indicate that some fuel from the downstream injector is entrained upstream by the recirculating flow behind the step. This upstream entrainment of H_2 from the downstream injector is also indicated by the regions of high and low temperature at location E. The fuel rich regions have a lower temperature because the H_2 is cold and because the fuel-air mixture is too rich to

react. At locations F and G, which are downstream of the primary fuel injector, large regions of unreacted fuel can be seen. With the present flow conditions, the H_2 injected from the primary injectors penetrates very well, passing beyond the combustor centerline [58].

Calculations are continuing with the Uenishi code to model complex three-dimensional combustor flow fields. A major effort is now also underway to compare the code with additional experimental data that has recently become available. Work is also currently being completed to couple the spatially elliptic Uenishi code to several parabolized Navier-Stokes programs, including the Chitsomboon PNS code and the Kamath PNS code, that were described earlier in this chapter. Parabolized Navier-Stokes codes can be more efficient for simulating the combustor far-field well away from the fuel injectors where the flow is spatially elliptic due to separation. Therefore, there is an incentive, based on computational efficiency, to switch to PNS programs wherever possible in the combustor.

A number of interesting combustor calculations have been made by Gielda using his three-dimensional parabolized Navier-Stokes program, SSCPNS, that was also described earlier in this chapter. One configuration that he analyzed is given in figure 18, which shows a sketch of a generic hypersonic propulsion system including an inlet, combustor, and nozzle [67]. Conditions entering the inlet were determined by assuming that the hypersonic vehicle was cruising at Mach 16 and at an altitude resulting in a free stream temperature and pressure of 452 R and 0.004 atm, respectively. Gaseous H_2 fuel was injected through five injectors into the engine beginning at a location x/L = 0.625 and continuing for a distance of x/L = 0.24 along the combustor as indicated by figure 18. This injection schedule resulted in a fuel equivalence ratio of approximately three. The fuel was injected at an angle of 25 degrees to the engine cowl defined in the figure by the x-axis.

Once the engine geometry and fuel injection configuration had been defined, the entire engine flow field was simulated using the SSCPNS code. The computed flow field was

highly three-dimensional. The three-dimensionality can be seen in figure 19 which shows Mach number contours at a number of cross-planes along the length of the inlet, combustor, and enclosed portion of the nozzle. Gielda's study also showed that there were significant losses associated with the fuel injection process in the generic engine. The losses resulted from the formation of strong oblique shocks as the inlet air interacted with the injected fuel. The induced shock waves can be seen in figure 20 which shows the computed pressure contours in the engine. The entropy increase that resulted when the engine flow passed through these oblique shocks caused a significant loss in the average stagnation pressure of the flow. This loss in stagnation pressure would ultimately result in a loss in the overall thrust that could be achieved. The fuel injector configuration did result, however, in good fuel-air mixing and combustion. The degree of combustion is indicated by the computed water mass fraction contours shown in figure 21 at several cross-planes along the combustor and nozzle lengths. Water mass fractions of up to 0.23 resulted across a large extent of the cross-planes, and an oxygen utilization of approximately 0.80 was achieved. Normalized static temperature contours in the engine resulting from the simulation are also shown in figure 21 [67].

In order to improve the performance of the engine, Gielda further investigated the fuel injection process in an attempt lower the associated shock losses. Three numerical experiments were performed that included a study of the engine flow field without injection or reaction, with injection, and with injection and reaction. By comparing the three cases, Gielda was able to assess the losses associated with the fuel injection process and associated with the heat addition resulting from the combustion process [67]. He concluded that further investigation into the injection process was required and that such a study would require simulation of the flow field near the fuel injectors using the spatially elliptic form of the Navier-Stokes equations. Such a study has recently been undertaken.

Carpenter used the SPARK3D spatially elliptic Navier-Stokes program, described earlier, to model the generic scramjet combustor sketched in figure 22 [59]. This combustor

configuration has been used as a generic model for actual combustor designs being considered as a part of a propulsion system for a hypersonic vehicle that will become operational early in the next century. Flow processed by an inlet enters the combustor from the left in the figure. The flow exits the inlet at a velocity of 1500 m/s, a static temperature of 1000 K, and a pressure of 0.5 atm. That flow then passes over rearward facing steps on the walls, experiencing a mild area expansion. Gaseous H_2 fuel is injected from a line of four orifice fuel injectors that lie along the face of the step on each of the four engine walls. The fuel and inlet air begin mixing just downstream of the steps. The flow for this configuration was simulated by Carpenter using the SPARK3D code [59]. Because the combustor was symmetric about its center, only the lower quadrant, shown in figure 22 was modeled. In addition, even though the program contained a generalized finite rate chemistry model, only fuel-air mixing was considered at this stage of the study. The resulting H_2 mass fraction distributions at 2 cm and 5 cm downstream of the step are given in figure 23. At the first station, recirculation behind the step and diffusion spread the hydrogen towards the walls, but there is little penetration of the fuel into the core flow in the center of the combustor. The 0.2 mass fraction contour does not extend beyond the height of the step. (Fuel rich regions having contours with a mass fraction greater than 0.2 were surpressed for clarity.) Further downstream at the 5 cm station, hydrogen mixes to a greater extent with the air, and the mixture extends further into the core flow. The extent of mixing is still not sufficient to provide an acceptable level of mixing efficiency or for that matter combustion efficiency if reaction had been allowed. As a result of these findings, mixing enhancement strategies similar to those discussed earlier are currently being applied to the generic combustor configuration to achieve an acceptable level of combustion efficiency.

Several other interesting calculations have also recently been undertaken to model scramjet combustor flow fields. But we have now reached the end of 1988, and it is time to bring this chapter to a conclusion. Computational methods have clearly been established as valuable tools for simulating combustor flows and providing an improved understanding

of their complex physics. Therefore, this story will continue to be told! With expected improvements in algorithms, computer resources, and creativity, the story should only improve, and computational methods should take on an even greater role in studying and designing high speed propulsion systems.

Concluding Remarks

Significant progress has been made in the past twenty years to develop techniques for modeling supersonic reacting flows. The progress has been due both to an advancement in numerical methods for computing reacting flow fields as well as an appreciable growth in computer speed and storage. The improvements in both algorithms and computer power have also lead to a gradually improved understanding of the physics of reacting flows *which is so very important if computation is to have a truly significant impact on scramjet combustor design.* The national program to develop a trans-atmospheric vehicle has been quite effective in generating a renewed interest in supersonic combustion, and it has spawned several programs aimed at better understanding its complexities. While these programs have begun to unravel some of the mysteries, they have also shown us that supersonic reacting flows still contain many unsolved questions. These questions provide exciting opportunities for future research, and these opportunities should not be missed!

The efficient mixing and combustion of fuel and air in a scramjet combustor remains a critical issue today. We are just beginning to understand the phenomena that suppress mixing in these high Mach number devices, but a great deal of work remains to be done. Once the mixing question is answered, many opportunities will still remain to employ this improved physical understanding to produce an efficient mixing strategy. Ground based experimental facilities will be used to study and design scramjet combustors by providing flows consistent with those that the engine will injest over its operating envelope. Ground based facilities are only able to create continuous flow conditions up to a flight Mach number of about 8, however. Beyond Mach 8, the only options available to the experimentalist

are pulse facilities that create flight conditions for only a short period of time, or the very vehicle that the national program seeks to build! Numerical methods provide an alternative to the Mach 8 barrier, but only if they are properly applied to the problem. To apply these methods properly, a fundamental understanding of the physical phenomena present in high speed reacting flows must be achieved. Even with this understanding, we will still be required to simulate flow fields in large geometric configurations, necessitating highly efficient numerical algorithms and significant advancements in computer technology. There is certainly a problem here for everyone! The problems are difficult ones, but they can be solved if we continue to tackle them in a careful and dedicated way. The United States committed itself to landing men on the moon in 1961, and it succeeded through a dedicated national commitment to do so in only eight short years. The national program to build and fly a trans-atmospheric vehicle is no more difficult a goal to achieve. It simply requires another national commitment to succeed, and a willingness on our part to accept the exciting challenges that such a program provides.

References

[1] Northam, G. B.; and Anderson, G. Y.: Supersonic Combustion Ramjet Research at Langley. AIAA Paper No. 86-0159, Jan. 1986.

[2] White, M. E.; Drummond, J. P.; and Kumar, A.: Evolution and Application of CFD Techniques for Scramjet Engine Applications. AIAA Journal of Propulsion and Power, v. 3, no. 5, Sep.-Oct. 1987, pp. 423-439.

[3] Walthrup, P. J. and Billig, F. S.: Liquid Fueled Supersonic Combustion Ramjets: A Research Perspective of the Past, Present, and Future. AIAA Paper No. 86-0158, Jan 1986.

[4] Billig, F. S.; Waltrup, P. J.; and Stockbridge, R. D.: Integral-Rocket Duel-Combustion Ramjets: A New Propulsion Concept. Journal of Spacecraft and Rockets, v. 17, Sep.-Oct. 1980.

[5] Ferri, A.: Mixing Controlled Supersonic Combustion. Annual Review of Fluid Mechanics, v. 5, 1973.

[6] Moretti, G.: Analysis of Two-Dimensional Problems of Supersonic Combustion Controlled by Mixing. AIAA Journal, v. 3, Feb. 1965, pp. 223-229.

[7] Edelman, R.; and Weilerstein, G.: A Solution of the Inviscid-Viscid Equations With Applications to Bounded and Unbounded Multicomponent Reacting Flows. AIAA Paper 69-83, Jan. 1969.

[8] Dash, S. M.: An Analysis of Internal Supersonic Flows with Diffusion, Dissipation, and Hydrogen-Air Combustion. NASA CR-111783, May 1970.

[9] Dash, S. M.; and DelGuidice, P. D.: Analysis of Supersonic Combustion Flowfields With Embedded Subsonic Regions. NASA CR-112223, Nov. 1972.

[10] Elghobashi, S. E.; and Spalding, D. B.: Equilibrium Chemical Reaction of Supersonic Hydrogen-Air Jets. NASA CR-2725, 1977.

[11] Spalding, D. B.; Launder, B. E.; Morse, A. P.; and Maples, G.: Combustion of Hydrogen-Air Jets in Local Chemical Equilibrium. NASA CR-2407, 1974.

[12] Markatos, N. C.; Spalding, D. B.; and Tatchell, D. G.: Combustion of Hydrogen Injected Into a Supersonic Airstream. NASA CR-2802, 1977.

[13] Patanker, S. V.; and Spalding, D. B.: A Calculation Procedure for Heat, Mass, and Momentum Transfer in Three-Dimensional Parabolic Flows. International Journal of Heat and Mass Transfer, v. 8, no. 15, pp. 1787-1806, 1972.

[14] Evans, J. S.; and Schexnayder, C. J.: Critical Influence of Finite Rate Chemistry and Unmixedness on Ignition and Combustion of Supersonic H_2-Air Streams. AIAA Paper No. 79-0355, Jan. 1979.

[15] Dash, S. M.; Sinha, N. and York B. J.: Implicit/Explicit Analysis of Interactive Phenomena in Supersonic Chemically Reacting Mixing and Boundary Layer Problems. AIAA Paper No. 85-1717, July 1985.

[16] MacCormack, R. W.: The Effect of Viscosity on Hypervelocity Impact Cratering. AIAA Paper No. 69-354, Apr. 1969.

[17] Briley, W. R. and McDonald, H.: Solution to the Multi-Dimensional Compressible Navier-Stokes Equations. Journal of Computational Physics, v. 24, pp.372-397, 1977.

[18] Beam, R. and Warming, R. F.: An Implicit Factored Scheme for the Compressible Navier-Stokes Equations. AIAA Journal, v. 16, no. 4 , pp. 393-402, 1978.

[19] Drummond, J. P.: Numerical Solution for Perpendicular Sonic Hydrogen Injection into a Ducted Supersonic Airstream. AIAA Journal, v. 17, no. 5, pp. 531-533, 1979.

[20] Drummond, J. P.: Numerical Investigation of the Perpendicular Injector Flow Field in a Hydrogen Fueled Scramjet. AIAA Paper No. 79-1482, June 1979.

[21] Drummond, J. P.; and Weidner, E. H.: A Numerical Study of Candidate Transverse Fuel Injector Configurations in the Langley Scramjet Engine. Seventeenth JANNAF Combustion Meeting, Hampton, VA, Sep. 22-26, 1980.

[22] Drummond, J. P.; and Weidner, E. H.: Numerical Study of a Scramjet Engine Flow Field. AIAA Paper No. 81-0186, Jan. 1981. Also AIAA Journal, v. 20, no. 9, pp. 1182-1187, 1982.

[23] Weidner, E. H.; and Drummond, J. P.: Numerical Study of Staged Fuel Injection for Supersonic Combustion. AIAA Paper No. 81-1468, July 1981. Also AIAA Journal, v. 20, no. 10, pp. 1426-1431, 1982.

[24] Schetz, J. A.: Turbulent Mixing of a Jet in a Co-Flowing Stream. AIAA Journal, v. 6, no. 10, pp. 2008-2010, 1968.

[25] Schetz, J. A.; Billig, F. S.; and Favin, S.: Analysis of Mixing and Combustion in a Scramjet Combustor with a Coaxial Fuel Jet. AIAA Paper No. 80-1256, June 1980.

[26] Schetz, J. A.; Billig, F. S.; and Favin, S.: Flowfield Analysis of a Scramjet Combustor with a Coaxial Fuel Jet. AIAA Journal, v. 20, no. 9, pp. 1268-1274, 1982.

[27] Griffin, M. D.; Billig, F. S.; and White, M. E.: Applications of Computational Techniques in the Design of Ramjet Engines. Presented at the 6th International Symposium on Air Breathing Engines, Paris, France, June 6-10, 1983.

[28] Williams, F. A.: *Combustion Theory.* Addison-Wesley Publishing Company, Inc., Reading, MA, pp. 358-429, 1965.

[29] McBride, B. J.; Heimel,S.; Ehlers, J. G.; and Gordon, S.: Thermodynamic Properties to 6000 K for 210 Substances Involving the First 18 Elements. NASA SP-3001, 1963.

[30] Kanury, A. M.: *Introduction to Combustion Phenomena.* Gordon and Breach Science Publishers, New York, pp. 363-371, 1982.

[31] White, F. M.: *Viscous Fluid Flow.* McGraw-Hill Inc., New York, pp. 28-36, 1974.

[32] Suehla, R. A.: Estimated Viscosities and Thermal Conductivities of Gases at High Temperature. NASA TR R-132, 1962.

[33] Wilke, C. R.: A Viscosity Equation for Gas Mixtures. Journal of Chemistry and Physics, v. 18, no. 4, pp. 517-519, 1950.

[34] Berman, H. A.; Anderson, J. D.; and Drummond, J. P.: Supersonic Flow Over a Rearward Facing Step with Transverse Nonreacting Hydrogen Injection. AIAA Journal, v. 21, no. 12, pp. 1701-1713, 1983.

[35] Kee, R. J.; Warnatz, J.; and Miller, J. A.: A Fortran Computer Code Package for the Evaluation of Gas-Phase Viscosities, Conductivities, and Diffusion Coefficients. Sandia Report SAND83-8209, Mar. 1983.

[36] Cebeci, T.; and Smith, A. M. O.: *Analysis of Turbulent Boundary Layers.* Academic Press, New York, 1974.

[37] Baldwin, B. S.; and Lomax, H.: Thin Layer Approximations and Algebraic Model for Separated Turbulent Flows. AIAA Paper No. 78-257, Jan. 1978.

[38] Jones, W. P.; and Launder, B. E.: The Prediction of Laminarization with a Two-Equation Model of Turbulence. International Journal of Heat and Mass Transfer, v. 15, p. 301, 1972.

[39] Fabris, G. ; Harsha, P. T.; and Edelman, R. B.: Multiple-Scale Turbulence Modeling of Boundary Layer Flows for Scramjet Applications. NASA CR-3433, 1981.

[40] Hanjalic, K.; and Launder, B. E.: Sensitizing the Dissipation Equation to Irrotational Strains. Journal of Fluids Engineering, Transactions of ASME, v. 102, pp. 34-40, 1980.

[41] Hanjalic, K.; Launder, B. E.; and Schiestel, R.: Multiple-Time Scale Concepts in Turbulent Transport Modeling. Second Sympsoium on Turbulent Shear Flows, Imperial College, London, July 1979.

[42] Rodi, W.: The Prediction of Free Turbulent Boundary Layers by Use of a Two-Equation Model of Turbulence. Ph.D. Thesis, University of London, 1972.

[43] Sindir, M. M.: Numerical Study of Turbulent Flows in Backward-Facing Step Geometries: Comparison of Four Models of Turbulence. Ph.D. Thesis, University of California, Davis, June 1982.

[44] Riley, J. J.; Metcalfe, R. W.; and Orszag, S. A.: Direct Numerical Simulations of Chemically Reacting Turbulent Mixing Layers. Physics of Fluids, v. 29, no. 2, pp. 406-422, 1986.

[45] Riley, J. J.; and Metcalfe, R. W.: Direct Numerical Simulations of Chemically Reacting Turbulent Mixing Layers. AIAA Paper No. 85-0321, Jan. 1985.

[46] McMurtry, P. A.; Jou, W.-H.; Riley, J. J.; and Metcalfe, R. W.: Direct Numerical Simulations of a Reacting Mixing Layer with Chemical Heat Release. AIAA Journal, v. 24, no. 6, pp. 962-970, 1986.

[47] Erlebacher, G.; and Hussaini, M.Y.: Stability and Transition in Supersonic Boundary Layers. AIAA Paper No. 87-1416, June 1987.

[48] Schumann, U.: Subgrid Scale Model for Finite Difference Simulations of Turbulent Flows in Plane Channels and Annuli. Journal of Computational Physics, v. 18, pp. 376-404, 1975.

[49] Speziale, C. C.; Erlebacher, G.; Zang, T. A.; and Hussaini, M. Y.: On the Subgrid-Scale Modeling of Compressible Turbulence. NASA CR-178420 (ICASE Report No. 87-73), 1987.

[50] Bussing, T. R. A.; and Murman, E. M.: A Finite Volume Method for Calculation of Compressed Chemically Reacting Flows. AIAA Paper No. 85-0311, Jan. 1985.

[51] Widhopf, G. F.; and Victoria, K. J.: On the Solution of the Unsteady Navier-Stokes Equations Including Multicomponent Finite Rate Chemistry. Computers and Fluids, v. 1, pp. 159-184, 1973.

[52] Drummond, J. P.; Rogers, R. C.; and Hussaini, M. Y.: A Detailed Numerical Model of a Supersonic Reacting Mixing Layer. AIAA Paper No. 86-1427, June 1986.

[53] Uenishi, K.; and Rogers, R. C.: Three-Dimensional Computation of Mixing of Transverse Injectors in a Ducted Supersonic Airstream. AIAA Paper No. 86-1423, June 1986.

[54] Kumar, A.: Numerical Analysis of the Scramjet Inlet Flow Field Using the Three-Dimensional Navier-Stokes Equations. CPIA Publication 373, Feb. 1983.

[55] Kumar, A.: Numerical Simulation of Flow Through Scramjet Inlet Using a Three-Dimensional Navier-Stokes Code. AIAA Paper No. 85-1664, July 1985.

[56] Uenishi, K.; Rogers, R. C.; and Northam, G. B.: Three-Dimensional Computations of Transverse Hydrogen Jet Combustion in a Supersonic Airstream. AIAA Paper No. 87-0089, Jan. 1987.

[57] Rogers, R. C.; and Chinitz, W.: Using a Global Hydrogen-Air Combustion Model in Turbulent Reacting Flow Calculations. AIAA Journal, v. 21, no. 4, pp. 586-592, 1983.

[58] Uenishi, K. ; Rogers, R. C.; and Northam, G. B.: Three-Dimensional Numerical Predictions of the Flow Behind a Rearward-Facing Step in a Supersonic Combustor. AIAA Paper No. 87-1962, June 1987.

[59] Carpenter, M. H.: Three-Dimensional Extensions to the SPARK Combustion Code. NASP CP-5029, Paper No. 15, Oct. 1988.

[60] Carpenter, M. H.: A Generalized Chemistry Version of SPARK. NASA CR-4196, 1988.

[61] Chitsomboon, T.; and Northam, G. B.: A 3-D PNS Computer Code for the Calculation of Supersonic Combusting Flows. AIAA Paper No. 88-0438, Jan. 1988.

[62] Chitsomboon, T.: Numerical Study of Hydrogen-Air Supersonic Combustion By Using Elliptic and Parabolized Equations. PhD Dissertation, Old Dominion University, Norfolk, VA, May 1986.

[63] Chitsomboon, T.; Kumar, A. and Tiwari, S. N.: Numerical Study of Finite-Rate Supersonic Combustion Using Parabolized Equations. AIAA Paper No. 87-0088, Jan. 1987.

[64] Vigneron, Y. C.; Rakich, J. V.; and Tannehill, J. C.: Calculation of Supersonic Viscous Flow Over Delta Wings with Sharp Subsonic Leading Edges. AIAA Paper No. 78-1137, July 1978.

[65] Schiff, L. B.; and Steger, J. L.: Numerical Simulation of Steady Supersonic Viscous Flow. AIAA Paper No. 79-0130, Jan. 1979.

[66] Gielda, T.; and McRae, D.: An Accurate, Stable, Explicit, Parabolized Navier-Stokes Solver for High Speed Flows. AIAA Paper No. 86-1116, May 1986.

[67] Gielda, T. P.; Hunter, L. G.; and Chawner, J. R.: Efficient Parabolized Navier-Stokes Solutions of Three-Dimensional, Chemically Reacting Scramjet Flow Fields. AIAA Paper No. 88-0096, Jan. 1988.

[68] Boris, J. P.: A Fluid Transport Algorithm That Works. Computing as a Language of Physics. International Atomic Energy Agency, Vienna, Austria, pp. 171-189, 1971.

[69] Boris, J. P.; and Book, D. L.: Flux-Corrected Transport I: SHASTA — A Fluid

Transport Algorithm That Works. Journal of Computational Physics, v. 11, pp. 38-69, 1973.

[70] Oran, E. S.; and Boris, J. P.: *Numerical Simulation of Reactive Flow.* Elsever Science Publishing Company, Inc., New York, N.Y., pp. 264-298, 1987.

[71] Zalesak, S. T.: Fully Multidimensional Flux-Corrected Transport Algorithms for Fluids. Journal of Computational Physics, v. 31, pp. 335-362, 1979.

[72] MacCormack, R. W.: Current Status of Numerical Solutions of the Navier-Stokes Equations. AIAA Paper No. 85-0032, Jan. 1985.

[73] Steger, J. L.; and Warming, R. F.: Flux Vector Splitting of the Inviscid Gasdynamic Equations with Applications to Finite-Difference Methods. Journal of Computational Physics, v. 40, pp. 263-293, 1981.

[74] Candler, G. V.; and MacCormack, R. W.: Hypersonic Flow Past 3-D Configurations. AIAA Paper No. 87-0480, Jan. 1987.

[75] Candler, G. V.; and MacCormack, R. W.: The Computation of Hypersonic Ionized Flows in Chemical and Thermal Nonequilibrium. AIAA Paper No. 88-0511, Jan. 1988.

[76] Grossman, B.; and Walters, R. W.: An Analysis of Flux-Split Algorithms for Euler's Equations with Real Gases. AIAA Paper No. 87-1117, June 1988.

[77] van Leer, B.: Flux-Vector Splitting for the Euler Equations. *Lecture Notes in Physics*, v. 170, pp. 507-512, 1982.

[78] Roe, P. L.: Characteristic-Based Schemes for the Euler Equations. *Annual Reviews in Fluid Mechanics*, v. 18, pp. 337-365, 1986.

[79] Anderson, W. K.; Thomas, J. L.; and van Leer, B.: A Comparison of Finite-Volume Flux Vector Splittings for the Euler Equations. AIAA Paper No. 85-0122, Jan. 1985.

[80] Walters, R. W.; and Dwoyer, D. L.: An Efficient Iteration Strategy Based on Upwind/Relaxation Schemes for the Euler Equations. AIAA Paper No. 85-1529-CP, July 1985.

[81] Grossman, B.; and Cinnella, P.: The Development of Flux-Split Algorithms for Flows with Nonequilibrium Thermodynamics and Chemical Reactions. AIAA Paper No. 88-3596, July 1988.

[82] Grossman, B.; and Cinnella, P.: Flux-Split Algorithms for Flows with Nonequilibrium Chemistry and Vibrational Relaxation. ICAM Report 88-08-03, Virginia Polytechnic Institute and State University, Blacksburg, Virginia, Aug. 1988.

[83] Liu, Y.; and Vinokur, M.: An Analysis of Numerical Formulations of Conservation Laws. NASA CR-177489, June 1988.

[84] Liou, M. S.; van Leer, B.; and Shuen, J. S.: Splitting of Inviscid Fluxes for Real Gases. Journal of Computational Physics, Accepted for Publication.

[85] Liou, M. S.: A generalized Procedure for Constructing an Upwind-Based TVD Scheme. AIAA Paper No 87-0355, Jan. 1987.

[86] Yee, H. C.: Construction of Explicit and Implicit Symmetric TVD Schemes and Their Applications. NASA TM-86775, July 1985. Also Journal of Computational Physics, v. 68, pp. 151-179, 1987.

[87] Yee, H. C.; and Shinn, J. L.: Semi-Implicit and Fully Implicit Shock Capturing Methods for Hyperbolic Conservation Laws with Stiff Source Terms. AIAA Paper No. 87-1116-CP, June 1987.

[88] Yee, H. C.: Upwind and Symmetric Shock-Capturing Schemes. NASA TM-????, May 1987.

[89] Shinn, J. L.; and Yee, H. C.: Extension of a Semi-Implicit Shock- Capturing Algorithm for 3-D Fully Coupled Chemically Reacting Flows in Generalized Coordinates. AIAA Paper No. 87-1577, June 1987.

[90] Gnoffo, P. A.; McCandless, R. S.; and Yee, H. C.: Enhancements to Program LAURA for Computation of Three-Dimensional Hypersonic Flow. AIAA Paper No. 87-0280, Jan 1987.

[91] Gnoffo, P. A.; and Green, F. A.: A Computational Study of the Flow Field Surrounding the Aeroassist Flight Experiment Vehicle. AIAA Paper No. 87-1575, June 1987.

[92] Gnoffo, P. A.; Gupta, R. N.; and Shinn, J. L.: Conservation Equations and Physical Models for Hypersonic Air Flows in Thermal and Chemical Nonequilibrium. NASA TP-2867, 1988.

[93] Shuen, J. S.; and Yoon, S.: Numerical Study of Chemically Reacting Flows Using an LU Scheme. AIAA Paper No. 88-0436, Jan. 1988.

[94] Yu, S. T.; and Shuen, J. S.: Three-Dimensional Simulation of an Underexpanding Jet Interacting with a Supersonic Cross Flow. AIAA Paper No. 88-3181, July 1988.

[95] Abarbanel, S.; and Kumar, A.: Compact High Order Schemes for the Euler Equations. NASA CR-181625, Feb. 1988.

[96] Hussaini, M. Y.; Salas, M. D.; and Zang, T. A.: Spectral Methods for Inviscid, Compressible Flows. *Advances in Computational Transonics*, ed. W. G. Habashi, Pineridge Press, Swansea, 1983.

[97] Gottlieb, D.; and Orszag, S. A.: Numerical Analysis of Spectral Methods, Theory, and Applications. CBMS-NSF Regional Conference Series in Applied Mathematics, SIAM, 1977.

[98] Drummond, J. P.; Hussaini, M. Y.; and Zang, T. A.: Spectral Methods for Modeling Supersonic Chemically Reacting Flowfields. AIAA Journal, v. 24, no. 9, pp. 1461-1467, 1986.

[99] Drummond, J. P.; and Hussaini, M. Y.: Numerical Simulation of a Supersonic Reacting Mixing Layer. AIAA Paper No. 87-1325, June 1987.

[100] Evans, J. S.; Schexnayder, C. J.; and Beach, H. L.: Application of a Two-Dimensional Parabolic Computer Program to Prediction of Turbulent Reacting Flows. NASA TP-1169, 1978.

[101] Burrows, M. C.; and Kurkov, A. P.: Analytical and Experimental Study of Supersonic Combustion of Hydrogen in a Vitiated Airstream. NASA TM X-2828, 1973.

[102] Brown, G. L.; and Roshko, A.: On Density Effects and Large Structure in Turbulent Mixing Layers. Journal of Fluid Mechanics, v. 64, pt. 4, pp. 775-816, 1974.

[103] Papamoschou, D.; and Roshko, A.: Observations of Supersonic Free Shear Layers. AIAA Paper No. 86-0162, Jan. 1986.

[104] Oh, Y. H.: Analysis of Two-Dimensional Free Turbulent Mixing. AIAA Paper No. 74-594, June 1974.

[105] Hussaini, M. Y.; Collier, F.; and Bushnell, D. M.: Turbulence Alteration Due to Shock Motion. *Turbulent Shear-Layer/Shock-Wave Interactions*, J. Delery, ed., Springer-Verlag, pp. 371-381, 1986.

[106] Drummond, J. P.: A Two-Dimensional Numerical Simulation of a Supersonic, Chemically Reacting Mixing Layer. NASA TM-4055, 1988.

[107] Drummond, J. P.; and Mukunda, H. S.: A Numerical Study of Mixing Enhancement in Supersonic Reacting Flow Fields. AIAA Paper No. 88-3260, July 1988.

[108] Guirguis, R. H.; Grinstein, F. F.; Young, T. R.; Oran, E. S.; Kailasanath, K.; and Boris, J. P.: Mixing Enhancement in Supersonic Shear Layers. AIAA Paper No. 87-0373, Jan. 1987.

[109] Guirguis, R. H.: Mixing Enhancement in Supersonic Shear Layers: III. Effect of Convective Mach Number. AIAA Paper No. 88-0701, Jan. 1988.

[110] Kumar, A.; Bushnell, D. M.; and Hussaini, M. Y.: A Mixing Augmentation Technique for Hypervelocity Scramjets. AIAA Paper No. 87-1882, June 1987.

TABLE 1. - Finite-Rate Chemistry Model and Arrhenius Rate Coefficients for Each Reaction

Reaction number	Reaction	A	N	E, kJ/g-mole
1.	$H_2+O_2=OH+OH$	0.1700E+14	0.00	201.5
2.	$H+O_2=OH+O$	0.1420E+15	0.00	68.6
3.	$OH+H_2=H_2O+H$	0.3160E+08	1.80	12.78
4.	$O+H_2=OH+H$	0.2070E+15	0.00	57.5
5.	$OH+OH=H_2O+O$	0.5500E+14	0.00	29.3
6.	$H+OH=H_2O+M$	0.2210E+23	-2.00	0.0
7.	$H+H=H_2+M$	0.6530E+18	-1.00	0.0
8.	$H+O_2=HO_2+M$	0.3200E+19	-1.00	0.0
9.	$HO_2+OH=H_2O+O_2$	0.5000E+14	0.00	4.2
10.	$HO_2+H=H_2+O_2$	0.2530E+14	0.00	2.9
11.	$HO_2+H=OH+OH$	0.1990E+15	0.00	7.5
12.	$HO_2+O=OH+O_2$	0.5000E+14	0.00	4.2
13.	$HO_2+HO_2=H_2O_2+O_2$	0.1990E+13	0.00	0.0
14.	$HO_2+H_2= H_2O_2+H$	0.3010E+12	0.00	78.2
15.	$H_2O_2+OH=HO_2+H_2O$	0.1020E+14	0.00	7.9
16.	$H_2O_2+H=OH+H_2O$	0.5000E+15	0.00	41.9
17.	$H_2O_2+O=OH+HO_2$	0.1990E+14	0.00	24.7
18.	$M+H_2O_2=OH+OH$	0.1210E+18	0.00	190.4
For the single step reaction		0.5510E+15	0.00	30.2

Appendix

Nomenclature

A_j	:	reaction rate constant for jth reaction
b_i	:	body force of species i
C_i	:	concentration of species i
$\dot{C}_i$	:	time rate of change of C_i
c_p	:	specific heat at constant pressure
D_{ij}	:	binary diffusion coefficient
D_T	:	thermal diffusion coefficient
E	:	total internal energy; activation energy
$\vec{E}, \vec{F}, \vec{G}$	:	flux vectors in x, y, and z coordinate directions
f_i	:	mass fraction of species i
g_j	:	Gibbs energy of species i
G_R	:	Gibbs energy of reaction
h_i	:	enthalpy of species i
h_i^o	:	reference enthalpy of species i
$\vec{H}$	:	source vector
K_b	:	backward rate constant
K_f	:	forward rate constant
K_{eq}	:	equilibrium constant
M	:	Mach number
M_i	:	molecular weight of species i
n_i	:	moles of species i
ns	:	number of chemical species
nr	:	number of chemical reactions
p	:	pressure
$\dot{q}$	:	heat flux

R^o	:	universal gas constant
T	:	temperature
T_R	:	reference temperature = $298^o k$
T_ϵ	:	effective temperature
t	:	time
Δt	:	time step
$\vec{U}$	:	dependent variable vector
u	:	streamwise velocity
v	:	transverse velocity
$\tilde{u}_i$	:	streamwise diffusion velocity of species i
$\tilde{v}_i$	:	transverse diffusion velocity of species i
$\tilde{V}_i$	:	diffusion velocity vector of species i
$\dot{w}_i$	:	species production rate of species i
x	:	streamwise coordinate
y	:	transverse coordinate
X_i	:	mole fraction of species i
λ	:	second viscosity coefficient
γ_{ij}	:	stoichiometric coefficient; species i, reaction j
γ	:	ratio of specific heats
δ	:	Kronecker delta function
ρ	:	density
σ	:	normal stress
σ_{ij}	:	effective collision diameter
τ	:	shear stress
μ_i	:	laminar viscosity of species i
μ	:	mixture laminar viscosity
ξ	:	computational streamwise coordinate

η	:	computational transverse coordinate
Ω_D	:	diffusion collision integral

List of Figures

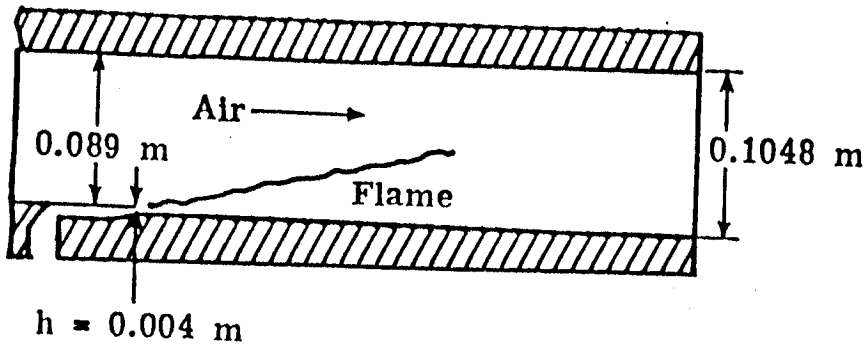
Air
0.089 m
Flame
0.1048 m
h = 0.004 m

FIG. 1

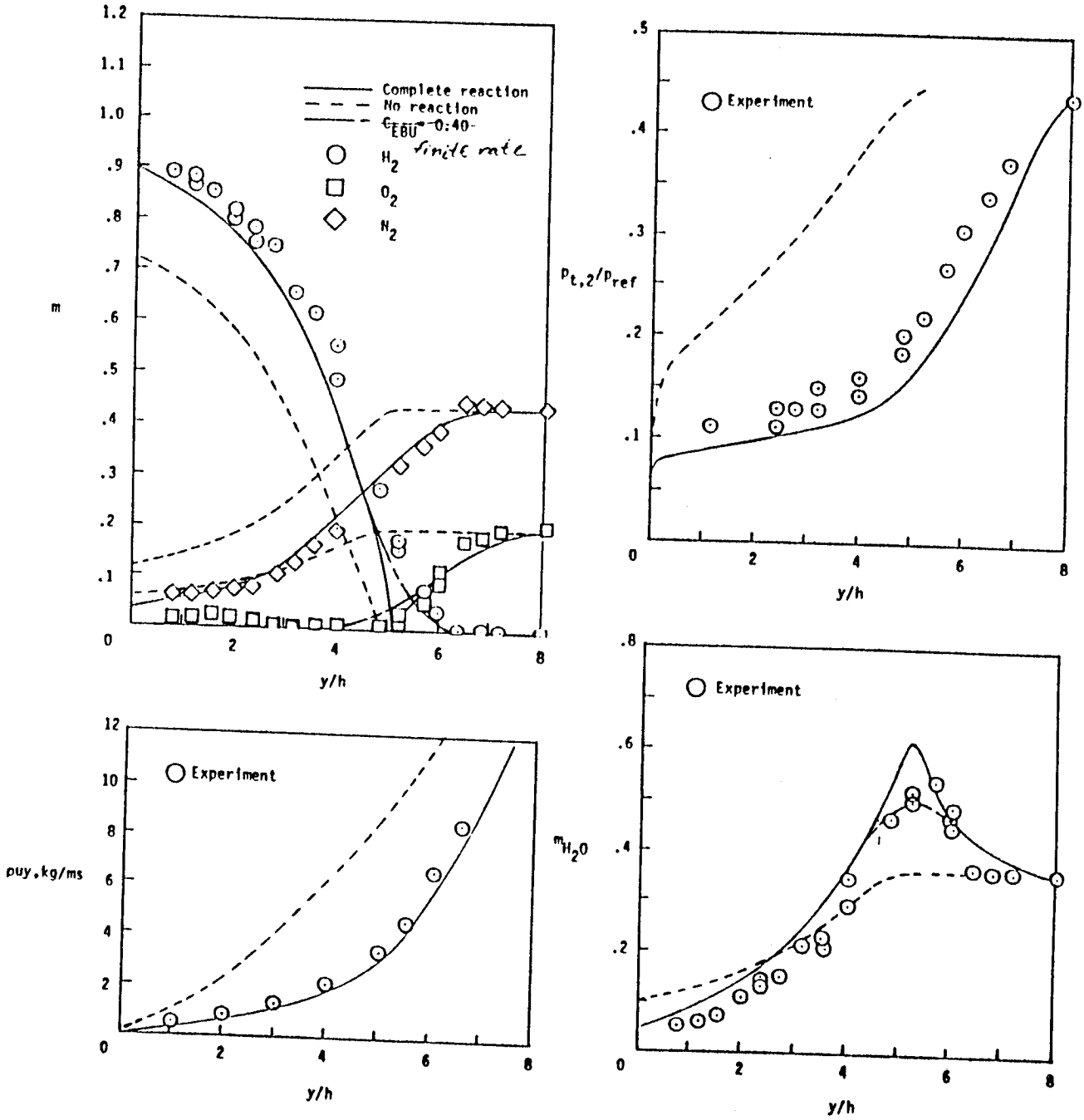
Complete reaction
No reaction
ϕ_{EQU} = 0.40
H_2
O_2
N_2
finite rate
m
y/h
Experiment
$p_{t,2}/p_{ref}$
y/h
Experiment
puy, kg/ms
y/h
Experiment
m_{H_2O}
y/h

FIG. 2

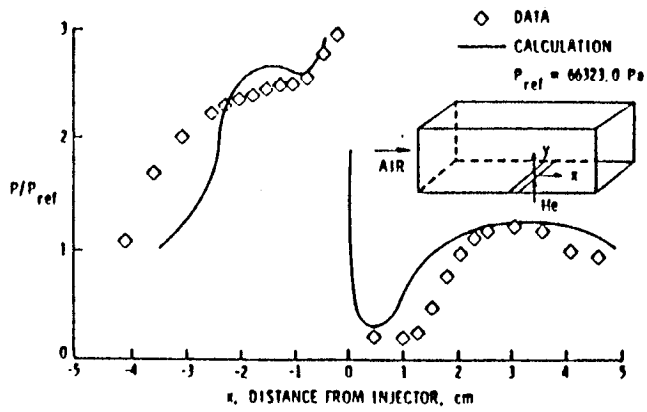

FIG. 3a.

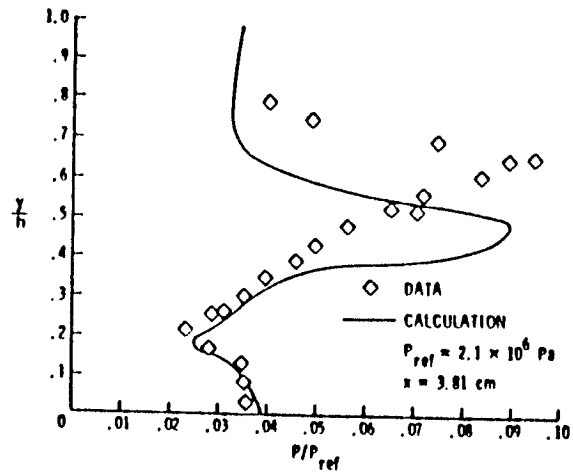

FIG 3b.

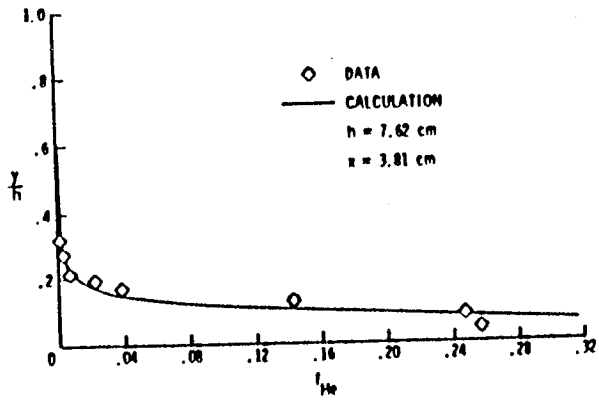

FIG. 3c.

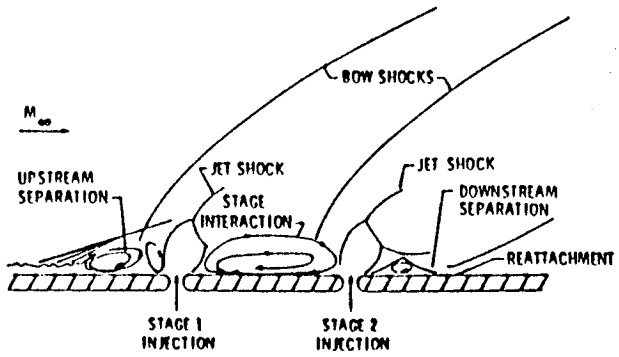

STAGED INJECTION FLOW FIELD SCHEMATIC

FIG. 4.

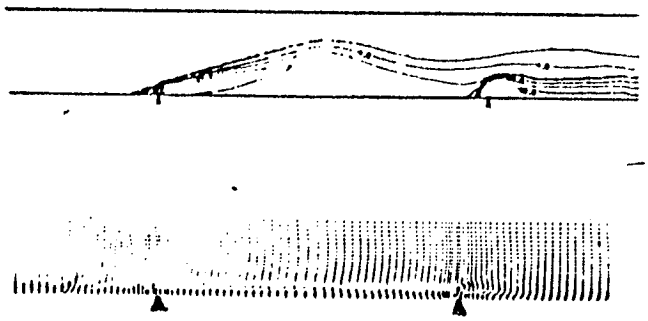

FIG. 5

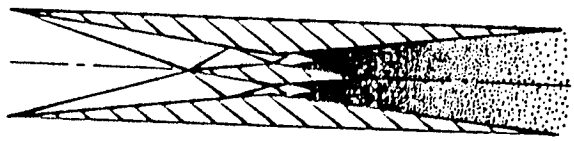

FIG. 6a.

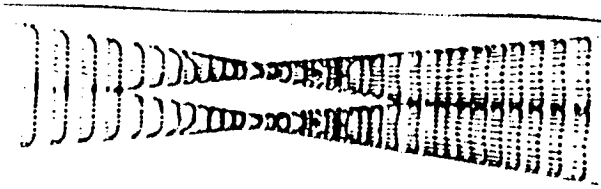

FIG. 6b.

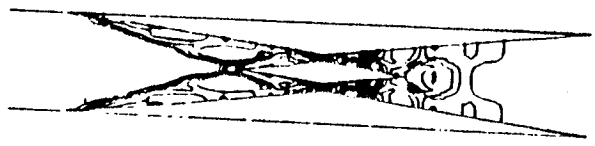

FIG. 6c.

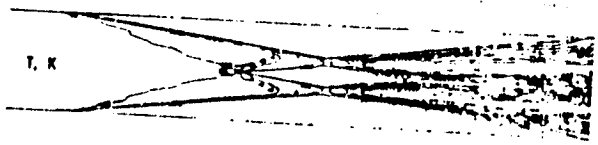

FIG. 6d.

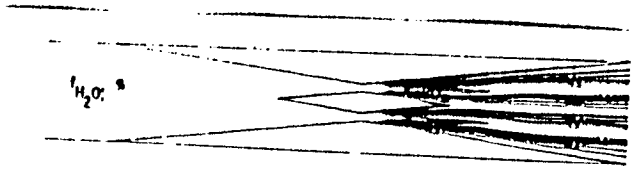

FIG. 6e.

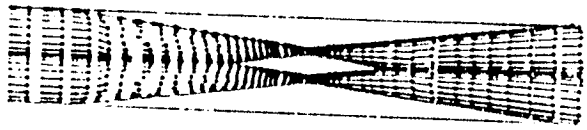

FIG. 7.

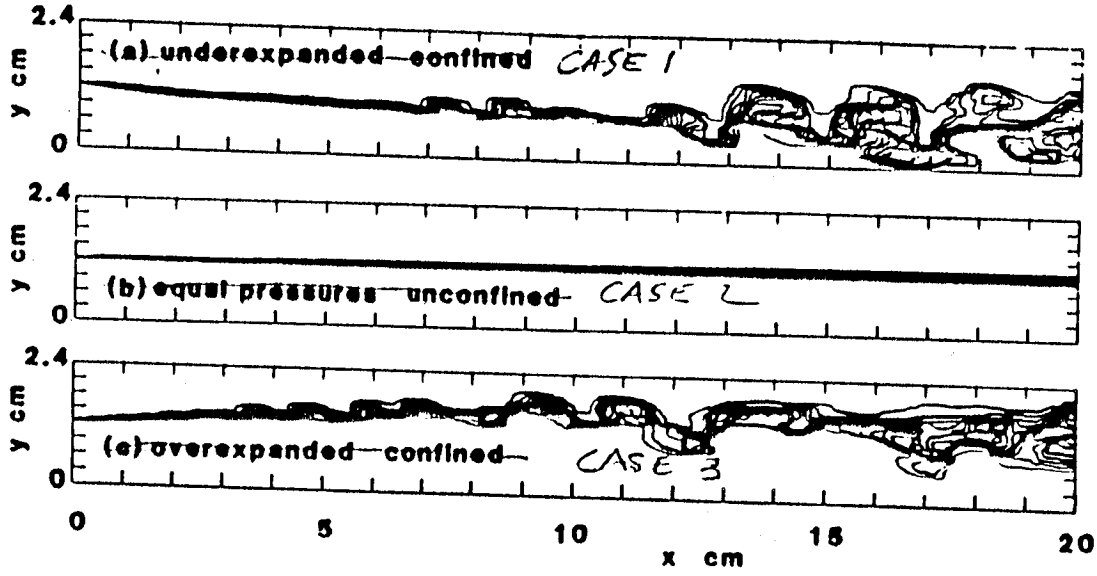

FIG. 8.

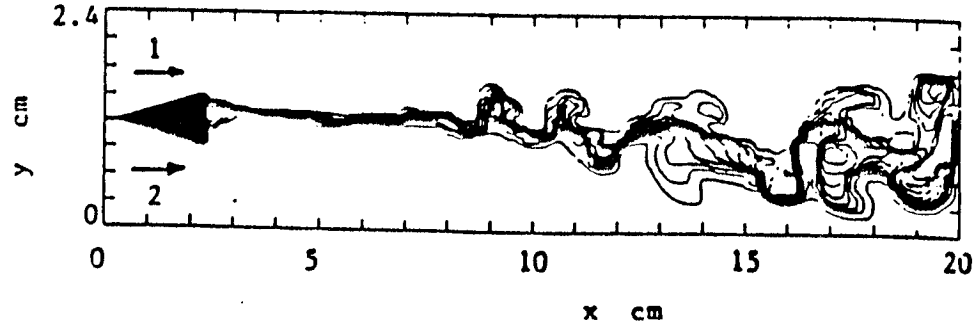

FIG. 9

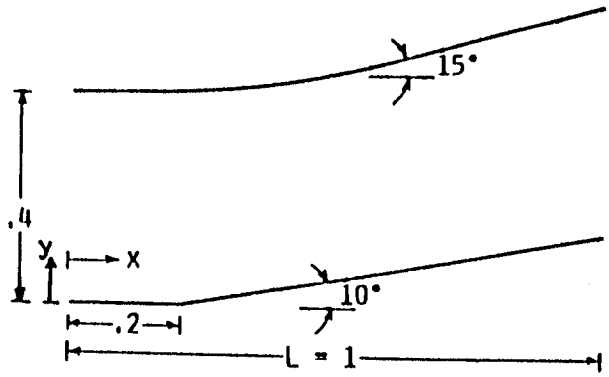

FIG. 10

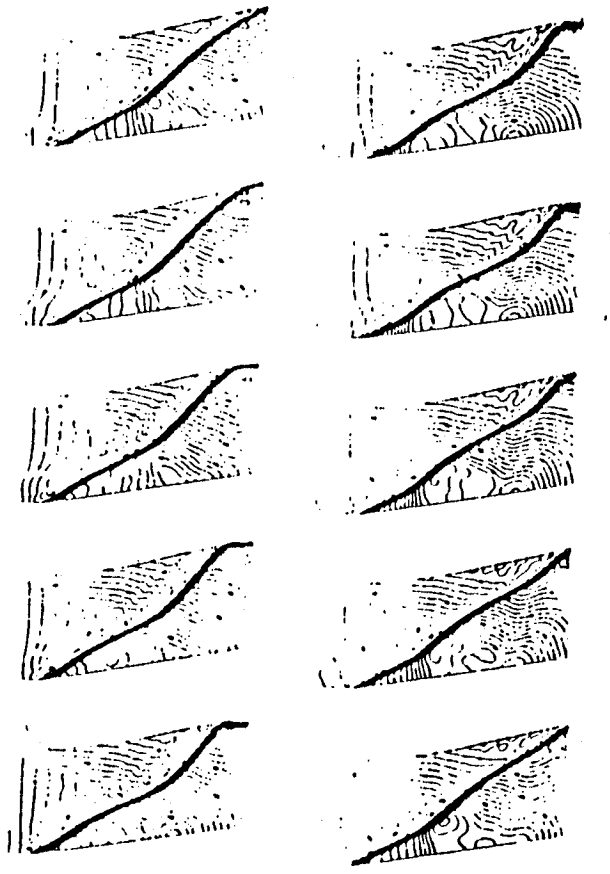

FIG. 11.

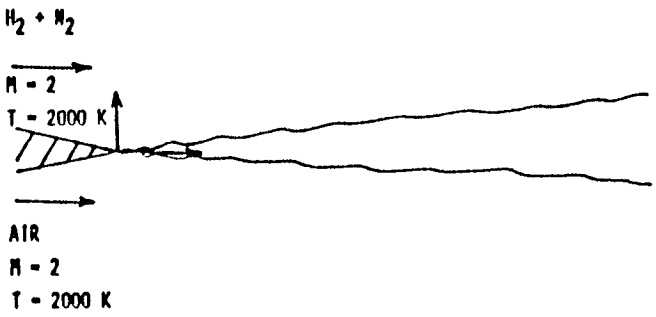

FIG. 12a.

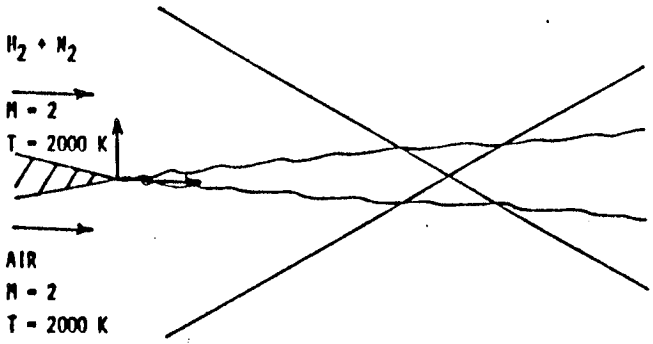

FIG. 12b.

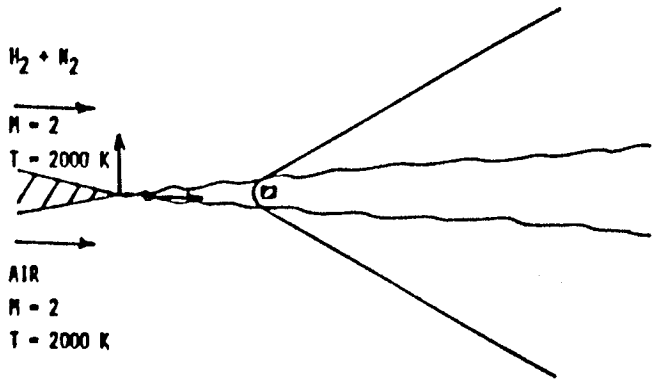

FIG. 12c.

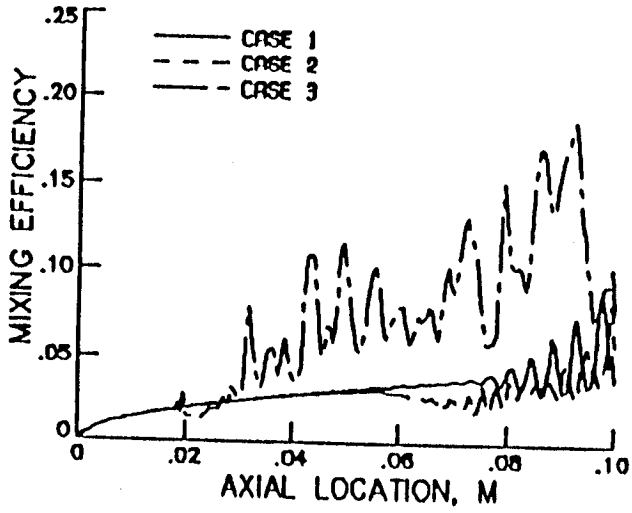

FIG. 13

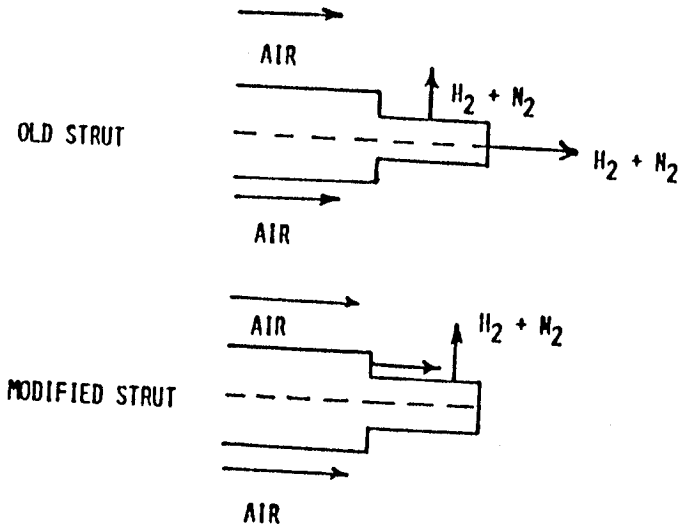

FIG 14a.

FIG. 14b.

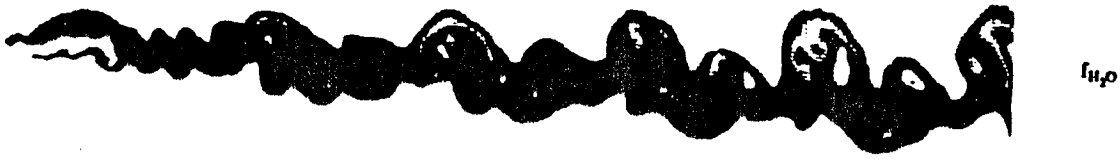

FIG. 14c.

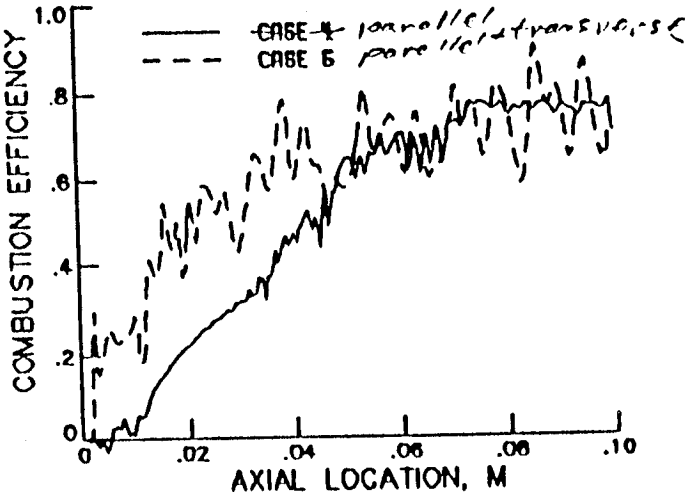
CASE 4 parallel/transverse
CASE 5 parallel
COMBUSTION EFFICIENCY
1.0
.8
.6
.4
.2
0
0
.02
.04
.06
.08
.10
AXIAL LOCATION, M

FIG. 15

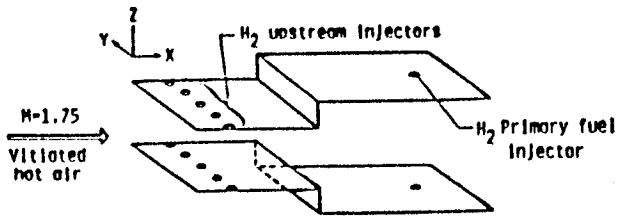

(a) Schematic of model combustor.

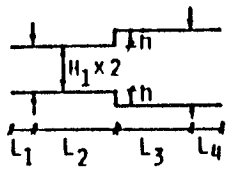

(b) View in X-Z plane

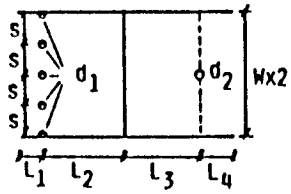

Injector diameters: d_1 = .132 cm, d_2 = .304 cm

Step height: h = .381 cm

H_1 = 5h L_1 = 3.41h L_2 = 12.33h L_3 = 9.67h

L_4 = 5.77 h S = 3.33h W = 6.66h

Injectors and Flow Conditions

Airstream: M_{FS} = 1.75 P_{FS} = 1.21 atm T_{FS} = 1212 K

$\delta_{B.L.}$ = 1.5h* n = .25

T_{wall} = 650 K

Upstream Injectors:

M_j = 1.0 P_j = 2.1 atm T_j = 250 K

A = .1 ρ_r = .57 C_d = .9

Downstream Injectors:

M_j = 1.0 P_j = 12.0 atm T_j = 250 K

A = .78 ρ_r = 3.2 C_d = .93

FIG. 16

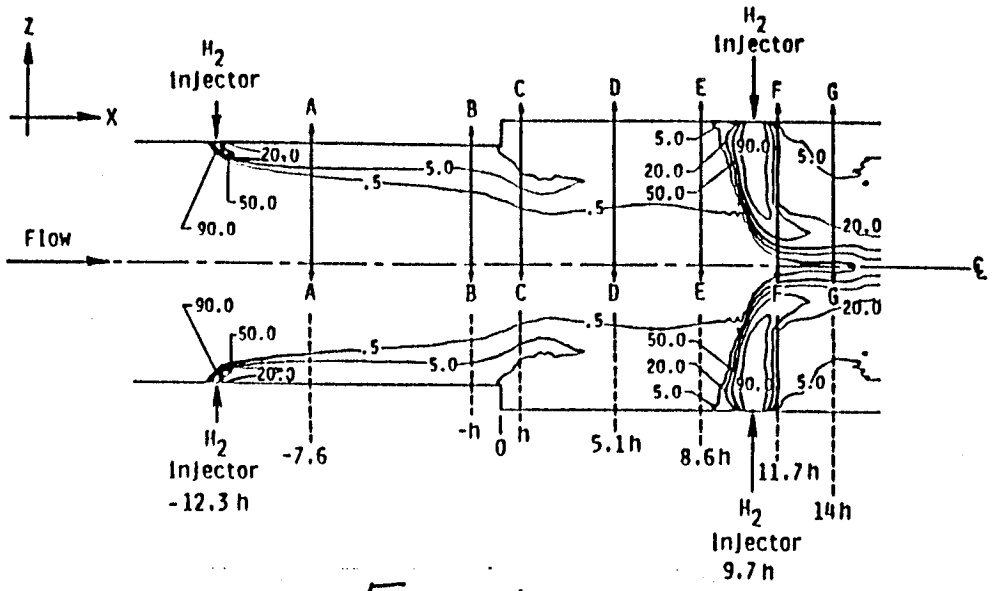

FIG. 17a

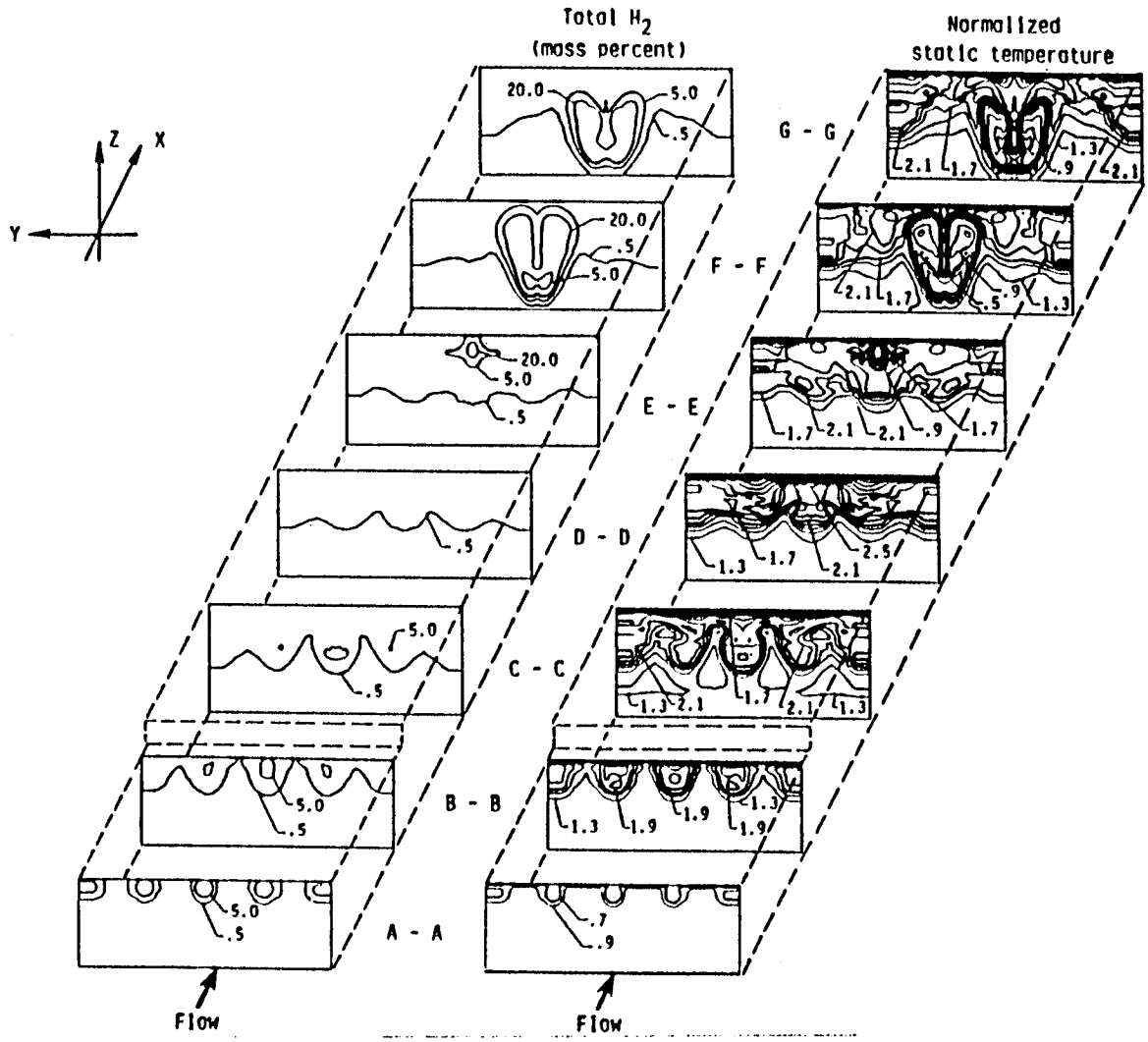

FIG 17b.

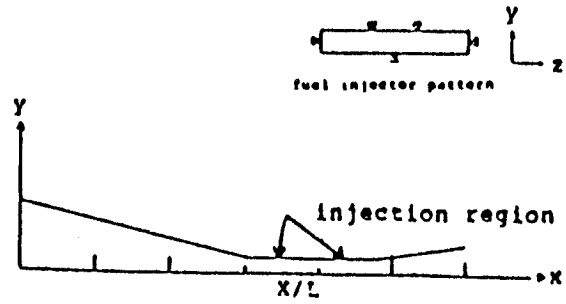

FIG. 18.

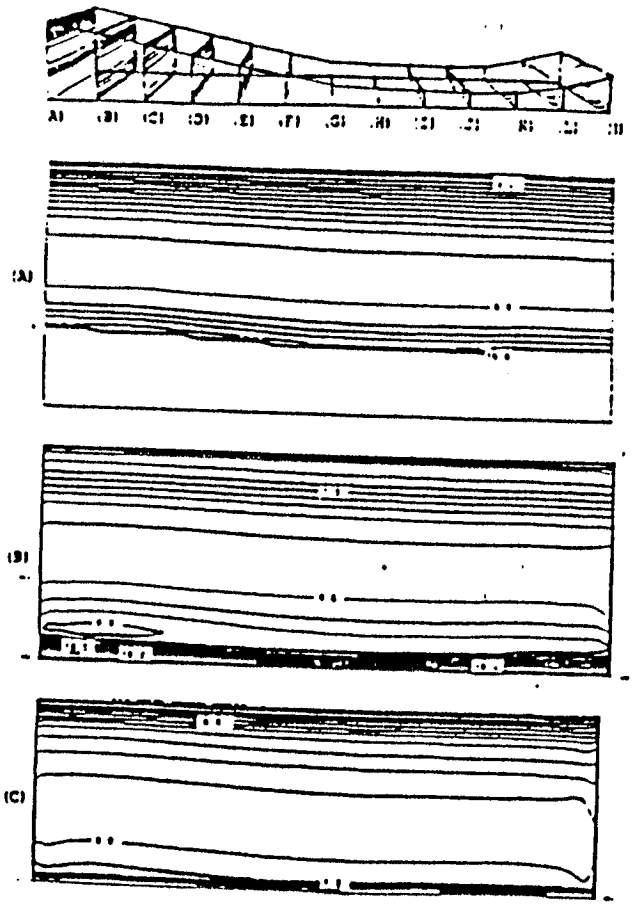

FIG. 19

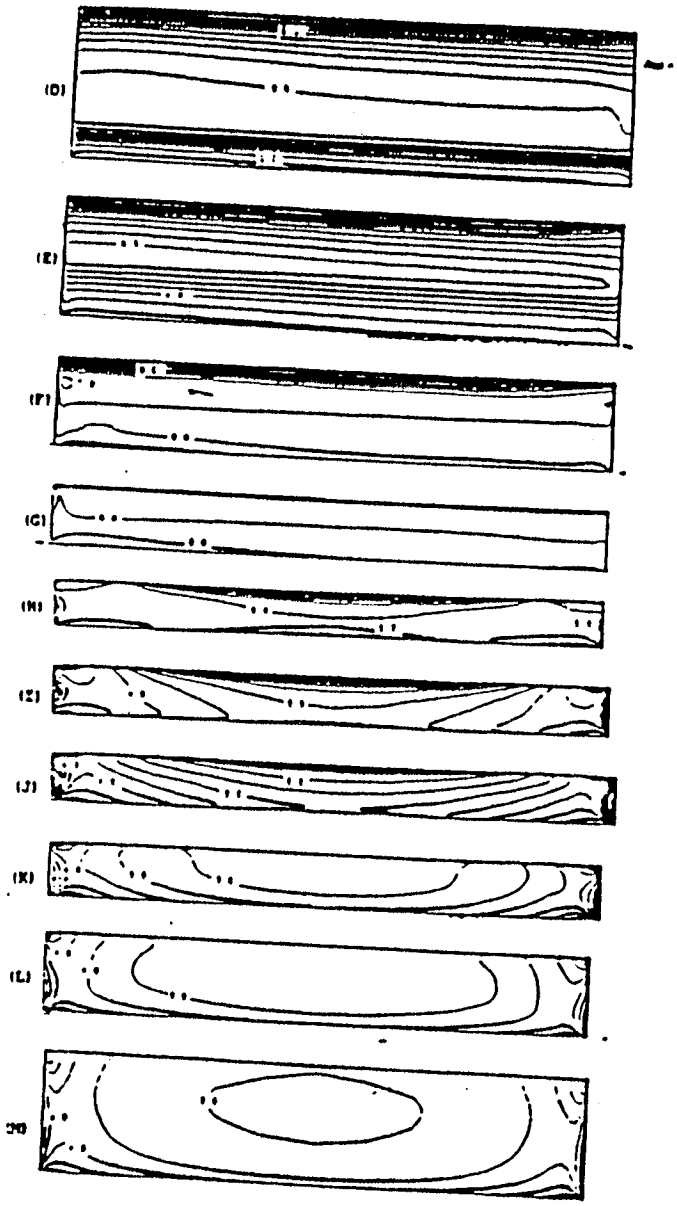

FIG. 19 (con't)

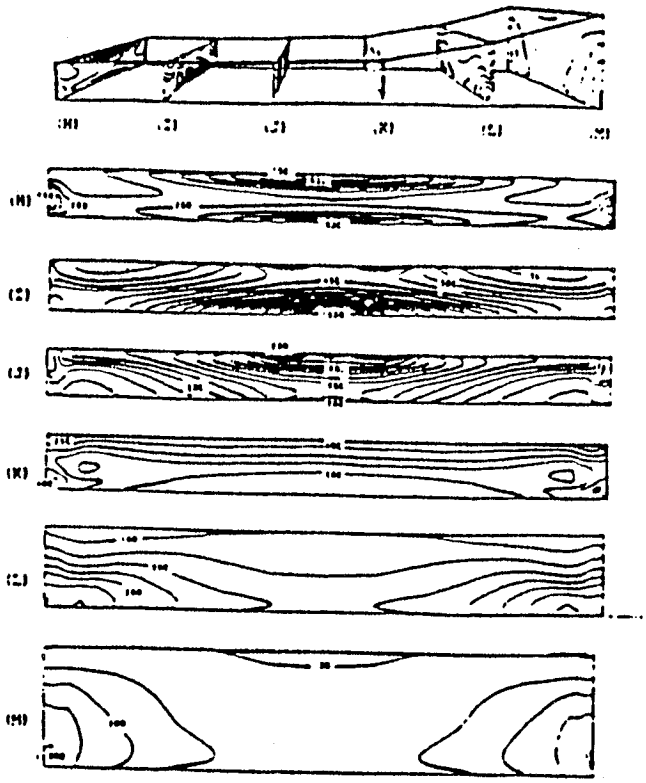

FIG. 20.

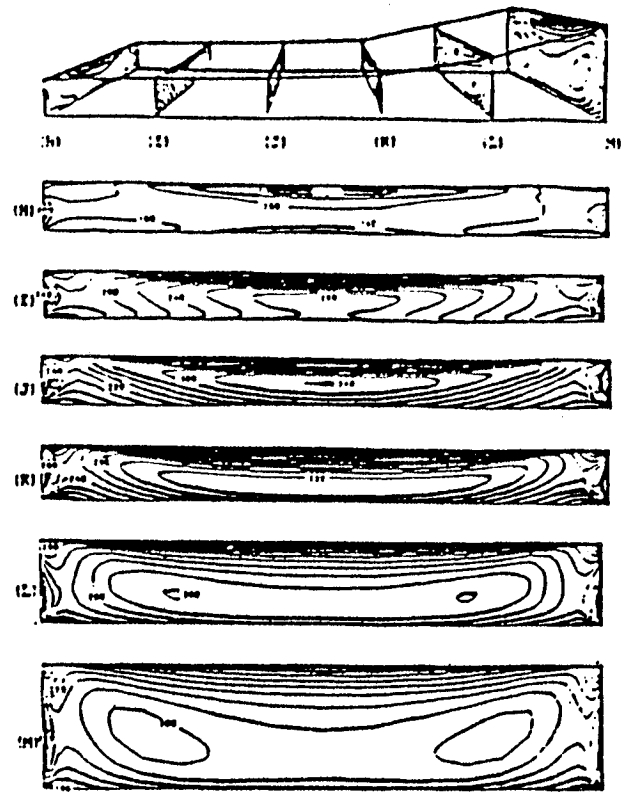

FIG. 21a.

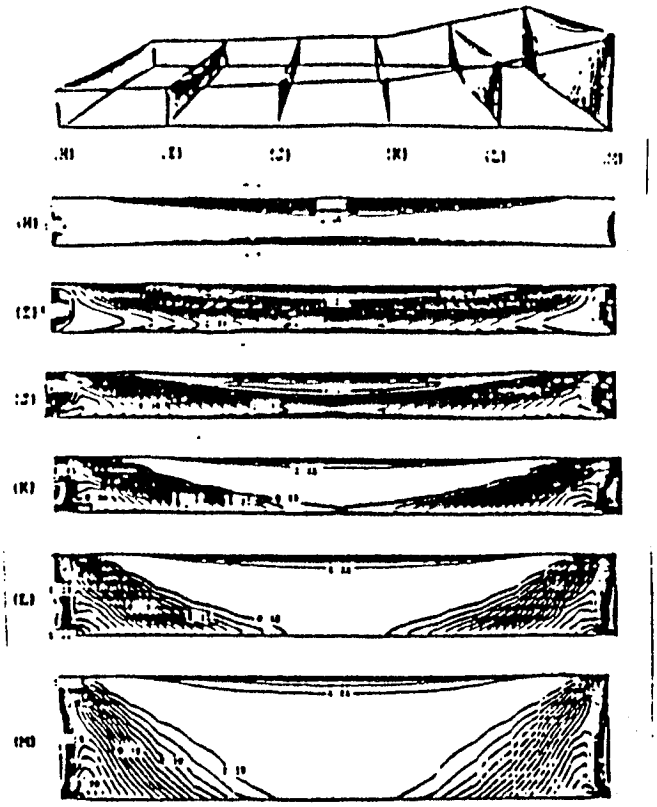

FIG 21b.

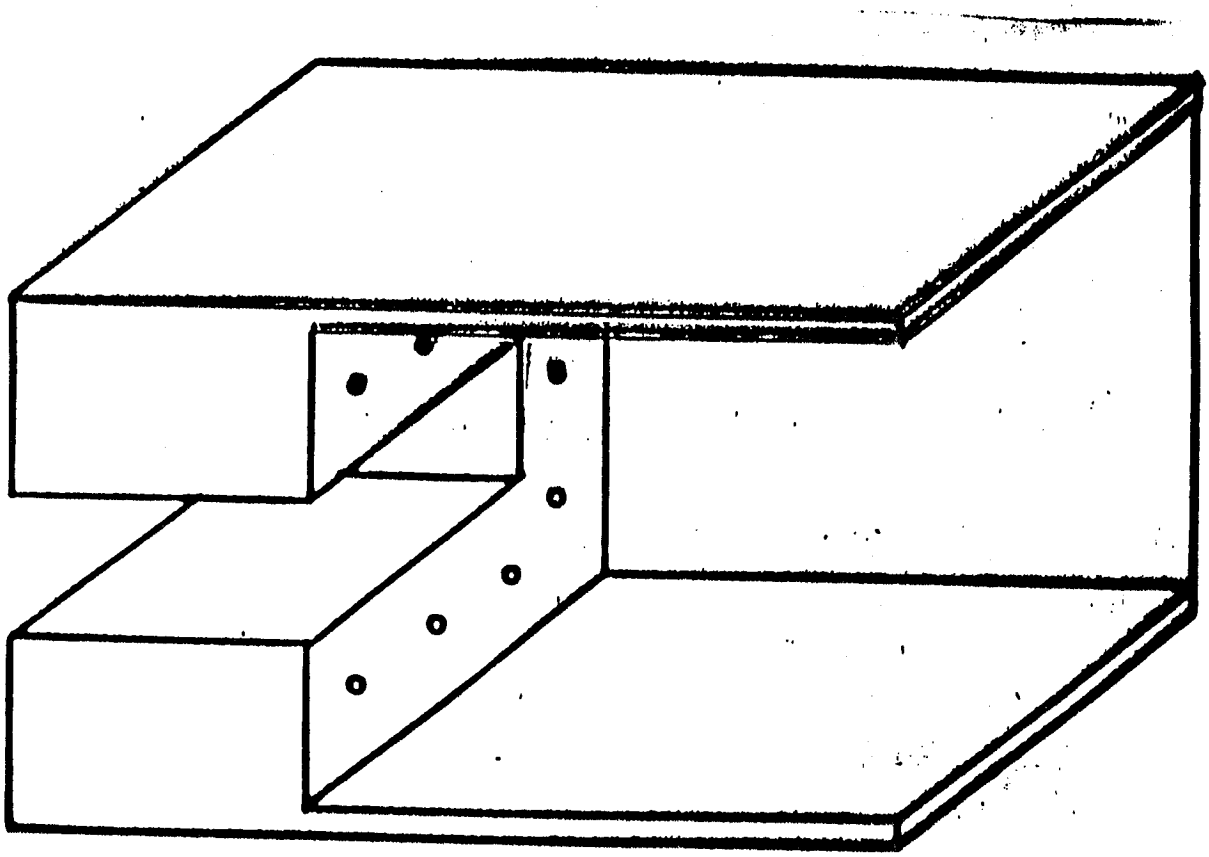

FIG. 22a.

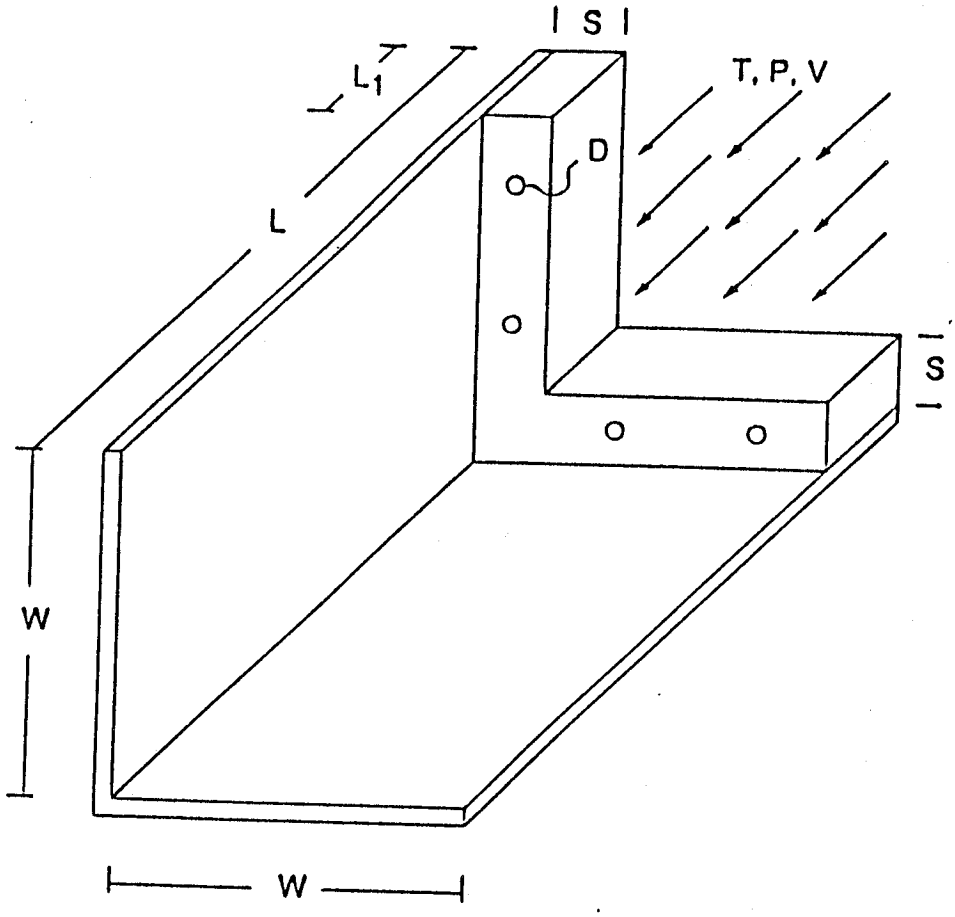

L = 20.0 cm, W = 10.0 cm
S = 2.0 cm, L_1 = 1.5 cm, D = 3.5 mm
T = 1000 K, P = 0.5 atm, V = 1500 m/s

FIG. 22b.

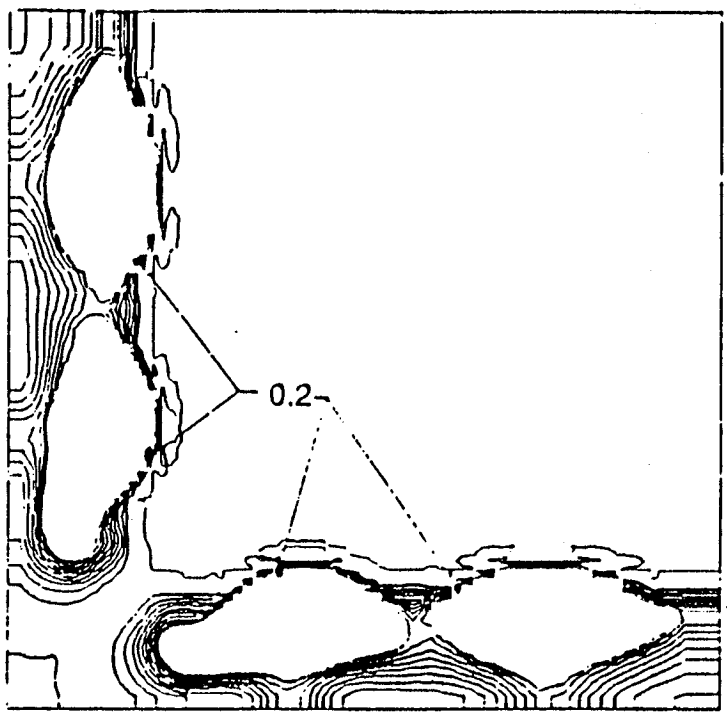

FIG. 23a.

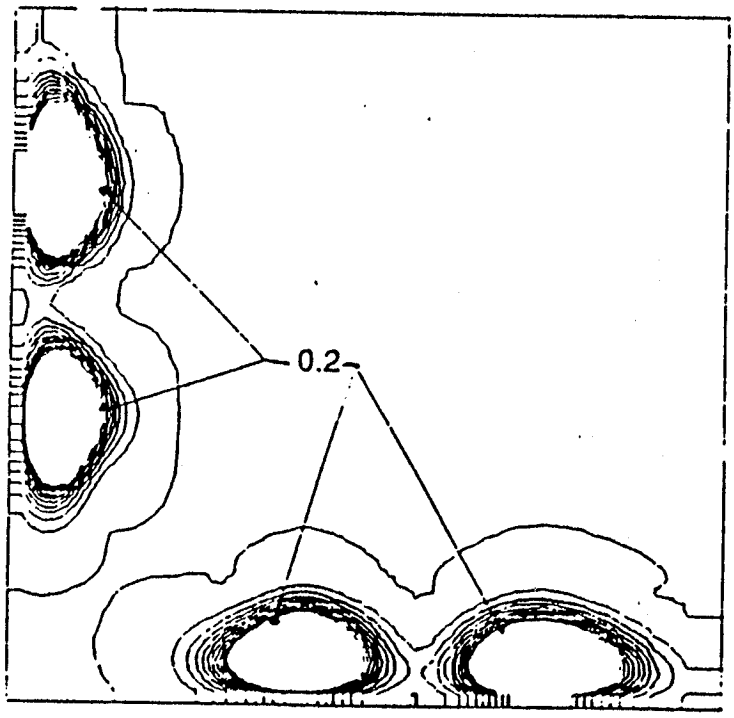

FIG. 23b.